Discovery of *N*-(4-(3-Amino-1*H*-indazol-4-yl)phenyl)-*N*′-(2-fluoro-5-methylphenyl)urea (ABT-869), a 3-Aminoindazole-Based Orally Active Multitargeted Receptor Tyrosine Kinase Inhibitor

Yujia Dai,*,[†] Kresna Hartandi,[†] Zhiqin Ji,[†] Asma A. Ahmed,[‡] Daniel H. Albert,[†] Joy L. Bauch,[†] Jennifer J. Bouska,[†] Peter F. Bousquet,[‡] George A. Cunha,[‡] Keith B. Glaser,[†] Christopher M. Harris,[‡] Dean Hickman,[†] Jun Guo,[†] Junling Li,[†] Patrick A. Marcotte,[†] Kennan C. Marsh,[†] Maria D. Moskey,[‡] Ruth L. Martin,[†] Amanda M. Olson,[†] Donald J. Osterling,[†] Lori J. Pease,[†] Niru B. Soni,[†] Kent D. Stewart,[†] Vincent S. Stoll,[†] Paul Tapang,[†] David R. Reuter,[†] Steven K. Davidsen,[†] and Michael R. Michaelides[†]

Global Pharmaceutical Research and Development, Abbott Laboratories, 100 Abbott Park Road, Abbott Park, Illinois 60064-6100, and Abbott Bioresearch Center, 100 Research Drive, Worcester, Massachusetts 01605-5314

Received November 2, 2006

In our continued efforts to search for potent and novel receptor tyrosine kinase (RTK) inhibitors as potential anticancer agents, we discovered, through a structure-based design, that 3-aminoindazole could serve as an efficient hinge-binding template for kinase inhibitors. By incorporating an *N,N*′-diaryl urea moiety at the C4-position of 3-aminodazole, a series of RTK inhibitors were generated, which potently inhibited the tyrosine kinase activity of the vascular endothelial growth factor receptor and the platelet-derived growth factor receptor families. A number of compounds with potent oral activity were identified by utilizing an estradiol-induced mouse uterine edema model and an HT1080 human fibrosarcoma xenograft tumor model. In particular, compound **17p** (ABT-869) was found to possess favorable pharmacokinetic profiles across different species and display significant tumor growth inhibition in multiple preclinical animal models.

Introduction

Angiogenesis, a process in which new blood vessels are formed from pre-existing vasculatures, is required for tumor growth and metastasis because blood is essential for solid tumors to manage nutritional supplies and waste removal. It has been shown that angiogenesis is a rate-limiting step in tumor development. Tumors that lack an adequate vasculature become necrotic or apoptotic and do not grow beyond a limited size. Consequently, inhibition of tumor angiogenesis has become a compelling approach in the development of anticancer agents.[1−3]

In tumor angiogenesis, vascular endothelial growth factor receptor tyrosine kinases are thought to play a prominent role by interacting with their extracellular ligands, vascular endothelial growth factors (VEGFs).[4] As a principal subfamily of receptor tyrosine kinases, VEGFRs (vascular endothelial growth factor receptors) are predominantly expressed in vascular endothelial cells and consist of FLT1 (Fms-like tyrosine kinase 1; VEGFR1), KDR (VEGFR2), and FLT4 (VEGFR3).[5,6] Overactivation of VEGFR family RTKs and, in particular, of KDR by VEGFs has been linked to the progression of a variety of human cancers. Studies have shown that VEGF-mediated KDR signaling induces a series of endothelial responses such as proliferation, migration, and survival and ultimately leads to new vessel formation and maturation. Due to the vital role that KDR signaling plays in tumor angiogenesis, compounds that have the ability to interrupt KDR signaling by targeting KDR or its ligands (VEGFs) have been pursued for the development of antiangiogenesis-based agents.[7−11] The approval by the FDA of Bevacizumab, a VEGF antibody, for the treatment of first-line metastatic colorectal cancer in combination with chemo-therapy has promoted even greater interest in this field. Several KDR-selective small molecule inhibitors, including **1** (PTK787)[12] (Figure 1), are in late-stage clinical trials.

Although VEGFRs play an important role in tumor growth and metastasis by means of angiogenesis, overactivation of other RTKs also contributes to tumor progression through a variety of mechanisms. One subfamily of these RTKs is the platelet-derived growth factor receptor tyrosine kinases, which are structurally related to the VEGFR family and include PDGFRα, PDGFR*β*, cKIT, CSF1R (colony-stimulating factor 1 receptor), and FLT3. PDGFR (platelet-derived growth factor receptor) kinases are believed to not only indirectly promote tumor angiogenesis, but also directly contribute to tumor growth by modifying the tumor microenvironment.[13−15] Additionally, the constitutive activation of FLT3 and cKIT by mutation is directly associated with the progression of acute myeloid leukemia (AML)[16] and gastrointestinal stromal tumor (GIST).[17]

As a result of the complex and redundant cellular signaling network associated with RTKs, broad-acting, multitargeted RTK inhibitors may be even more advantageous than selective agents, because these types of inhibitors have the ability to block multiple signaling pathways, upon which tumor survival depends.[18,19] This is evidenced by the FDA's recent approval of two multitargeted kinase inhibitors, **2** (SU11248)[20] and **3** (BAY 43-9006)[21] (Figure 1), as new agents for cancer treatment. While **2** targets both VEGFR and PDGFR tyrosine kinases, **3** also inhibits Raf kinase in addition to the VEGFR and PDGFR kinases.

In the search for novel and potent multitargeted RTK inhibitors, we recently identified a series of thienopyrimidine ureas (e.g., **5** in Figure 2) as potent inhibitors of all the kinases of both VEGFR and PDGFR families.[22] A number of compounds from this series were found to be orally efficacious in tumor growth models such as human HT1080 fibrosarcoma xenografts. The preliminary but promising results of this series

---

* To whom correspondence should be addressed. Dr. Yujia Dai, R47J/AP10, Cancer Research, 100 Abbott Park Road, Abbott Park, Illinois 60064. Tel.: (847) 937-8977. Fax: (847) 935-5165. E-mail: yujia.dai@abbott.com.
† Abbott Laboratories, Abbott Park, IL.
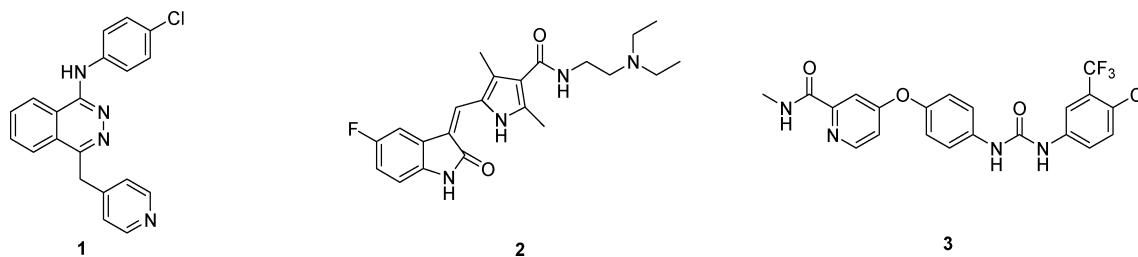‡ Abbott Bioresearch Center, Worcester, MA.

Figure 1. KDR-selective inhibitor **1** and multitargeted RTK inhibitors **2** and **3**.
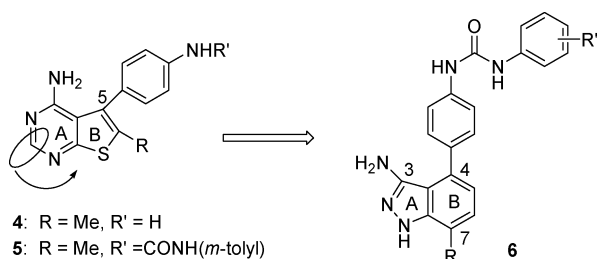

Figure 2. Rational design of 3-aminoindazole urea RTK inhibitors.
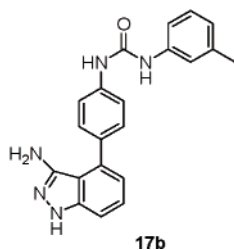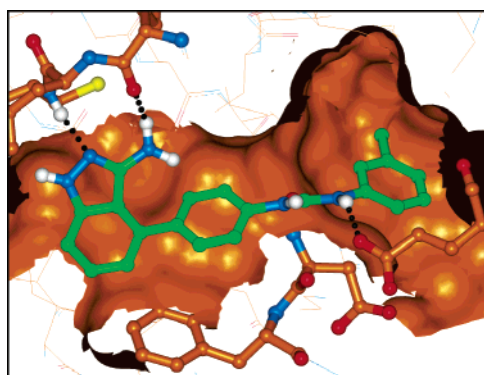

Figure 3. Model of **17b** bound to KDR kinase. Hydrogen bonds in black are shown between the urea external NH and Glu 885 carboxylate, between the 3-amino group of the indazole and Glu 917 backbone carbonyl, and between the ring nitrogen (N2) and Cys 919 NH. Also in thick bond are residues Asp 1046−Phe 1047 of the DFG motif in the inactive conformation (DFG-out).

inspired us to search for additional inhibitors with new chemotypes to target VEGFR and PDGFR kinases. Utilizing a rational design strategy, we were able to discover a new series of urea RTK inhibitors based on a 3-aminoindazole template (**6**, Figure 2). These 3-aminoindazole ureas proved to be potent inhibitors against the members of the VEGFR and PDGFR families. From this series, a clinical candidate, **17p** (ABT-869), was identified. In this paper, we report the rational design, chemical synthesis, and structure−activity relationships of this novel series as well as in vitro and in vivo properties of **17p**.

Inhibitor Design

In our studies of the thienopyrimidine series, a homology model of KDR bound to **5** suggested that the thienopyrimidine

nucleus in **5** mimicked the adenine component of ATP, forming a pair of hydrogen-bonding interactions with the KDR hinge region. The *N,N′*-diaryl urea portion extended into the hydrophobic back pocket of KDR kinase and contributed significantly to the inhibitors' KDR affinity. Considering the importance of the urea link for the potency of thienopyrimidine inhibitors, we decided to maintain the *N,N′*-diaryl urea portion in our new inhibitors and try to replace the thienopyrimidine pharmacophore with an alternative template. Such a template should possess two basic structural features: the capability to form hydrogen-bonding interactions with the KDR hinge region and an appropriate attachment vector for the diaryl urea, allowing for optimal interactions with the KDR hydrophobic pocket. With this working plan in mind, we envisioned that removal of the CH unit from the six-membered pyrimidine ring (A-ring) and insertion back into the five-membered B-ring, as shown in Figure 2, might satisfy both design criteria. This "CH-shift" strategy converted the 6-5 ring system of the thienopyrimidine into a 5-6 system, one permutation of which is the 3-aminoindazole (**6**). With its 3-amino group and the ring nitrogen (N2), the 3-aminoindazole unit should be able to mimic the adenine component of ATP to form a pair of hydrogen-bonding interactions with the KDR hinge region. The endocyclic NH unit might offer another site for a third hydrogen-bonding interaction with the kinase. Additionally, incorporation of the *N,N′*-diaryl urea at the C4-position of the indazole system should provide the required orientation for the urea to interact with the KDR back pocket.

To provide support to this rational design, a homology model of KDR bound to **5** (Figure 3) was created, following the same protocol as reported previously for the thienopyrimidine urea KDR inhibitors.[22] This model suggested that this new series of compounds represented by the general structure **6** would, as expected, bind to the ATP site of an inactive confirmation of KDR kinase (DFG-out confirmation). The 3-aminoindazole template indeed mimicked the adenine portion of ATP, interacting with the hinge region of KDR through hydrogen bonds between (1) the exocyclic amino (3-amino) group and the backbone carbonyl of Glu 917 and (2) the proximal ring nitrogen (N2) and the backbone NH of Cys 919. The urea portion accessed the back hydrophobic pocket adjacent to the ATP-binding site, with the urea carbonyl oxygen forming a hydrogen-bonding interaction with the backbone N−H of Asp 1046 of the DFG motif. The external NH of the urea link also formed a hydrogen-bonding interaction with the side chain carboxylate of Glu 885 of the αC helix. These suggested interactions between the urea unit and the back hydrophobic pocket of KDR were consistent with reports of other RTK inhibitors of the urea class[23,24] and matched well with the proposed binding model for the thienopyrimidine ureas. In fact, the modeling was able to generate an almost perfect overlap for **17b** and thienopyrimidine urea **5** (Figure 4).
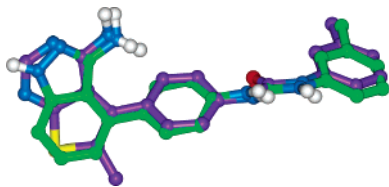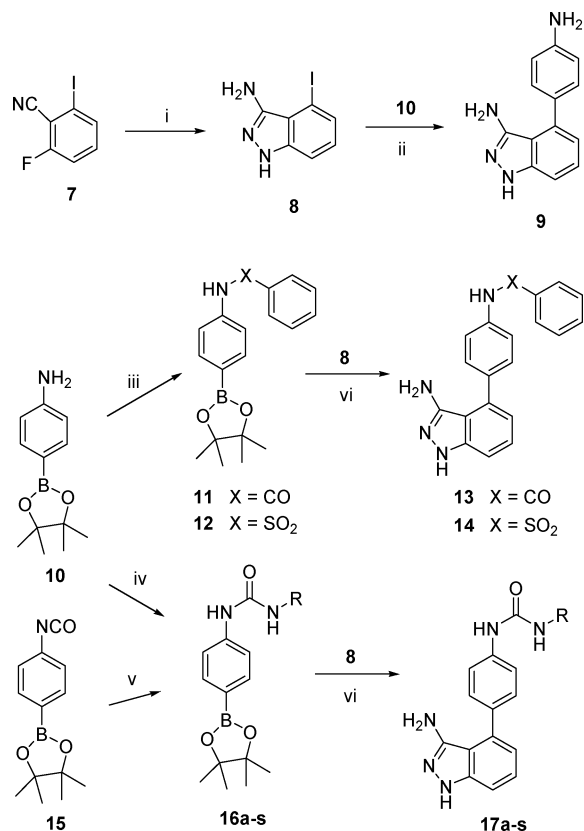
Figure 4. Overlap of 3-aminoindazole urea **17b** (in green) with thieopyrimidine urea **5** (in purple).

Scheme 1. Synthesis of 3-Aminoindazole Amide **13**, Sulfonamide **14**, and Ureas **17a**−**s**[a]

[a] Reagents and conditions: (i) NH$_2$NH$_2$·H$_2$O, *n*-BuOH, 110 °C, 90%; (ii) Pd(PPh$_3$)$_4$, Na$_2$CO$_3$, toluene, EtOH, H$_2$O, 90 °C, 60%; (iii) PhXCl, Et$_3$N, CH$_2$Cl$_2$, 0 °C → rt, 80−95%; (iv) RNCO, CH$_2$Cl$_2$, 0 °C → rt, 70−95%; (v) RNH$_2$, CH$_2$Cl$_2$, 0 °C → rt; (vi) Method A: Pd(dppf)Cl$_2$·CH$_2$Cl$_2$, Na$_2$CO$_3$, DME, H$_2$O, 85 °C; or method B: Pd(dppf)Cl$_2$·CH$_2$Cl$_2$, Na$_2$CO$_3$, DME, H$_2$O, microwave, 140−160 °C, 15−20 min.

Chemistry

A general synthesis of C4-substituted aminoindazoles is shown in Scheme 1. 3-Amino-4-iodoindazole (**8**) was easily prepared by reaction of 2-fluoro-6-iodobenzonitrile (**7**) with hydrazine monohydrate. The Suzuki coupling reaction between **8** and boronate **10** provided aniline **9**. Despite its easy access, **9** could not be used for the synthesis of ureas **17a**−**s** due to a competitive endocyclic *N*-acylation at NH-position (N1) of the indazole upon reaction with isocyanates. Consequently, ureas **17a**−**s** were synthesized by coupling **8** with urea boronates **16a**−**s**, which were prepared either via reaction of **10** with the corresponding isocyanates or via reaction of **15** with the corresponding amines. In a similar fashion, amide **13** and sulfonamide **14** were obtained from reaction of **8** with amide boronate **11** and sulfonamide boronate **12**, respectively.

Introduction of a substituent on the endocyclic NH (N1) of 3-aminoindazoles (**20a**−**d**) was accomplished by treating **7** with an alkyl hydrazine RNHNH$_2$ (R = Me, HOCH$_2$CH$_2$) or via alkylation of **18**, in which the 3-amino group was selectively
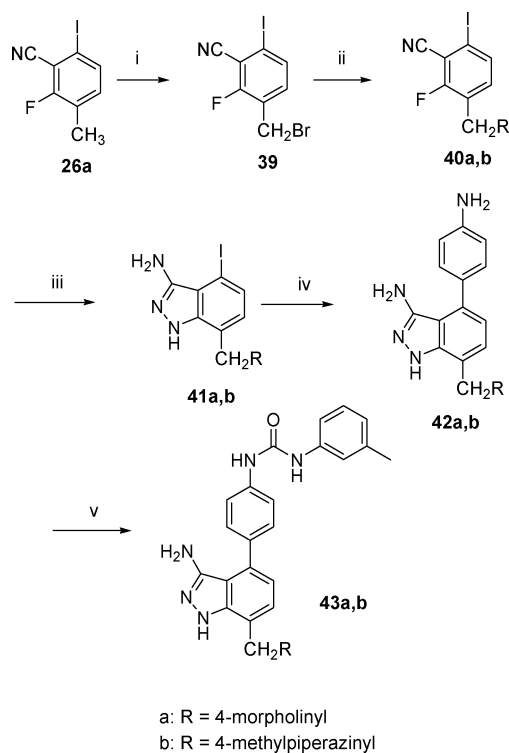
protected in the form of a phthalimide (Scheme 2). While ureas **22a**,**c**,**d** were conveniently synthesized via reaction of anilines **21a**,**c**,**d** with the corresponding aryl isocyanates, the Suzuki coupling reaction between iodide **20b** and urea boronate **16b** was chosen for the preparation of urea **22b** to avoid the potential side reaction of the alcohol functionality in aniline **21b** (not shown in Scheme **2**) with the isocyanate.

Analogs with a substituent at the 7-position of the aminoindazole were synthesized as outlined in Scheme 3. Fluoride-directed lithiation of **23a**−**d** with lithium diisopropylamide (LDA) and subsequent reaction with carbon dioxide yielded acids **24a**−**d**, which were then converted into amides **25a**−**d** via the corresponding acid chlorides. Dehydration of **25a**−**d** to form nitriles **26a**−**d** was carried out using thionyl chloride in warm dimethylformide (DMF). With nitriles **26a**−**d** in hand, anilines **28a**−**d** were readily synthesized via the cyclization with hydrazine followed by the Pd-mediated coupling. Unlike the case of aniline **9**, the 7-substituents on the indazole ring in **28a**−**d** sterically suppressed the competitive *N*-acylation reaction at the N1-position and allowed anilines **28a**−**d** to react with *m*-tolyl isocyanate to generate desired ureas **29a**−**d**.

Nitriles **26a** and **26b** not only served as the intermediates for the synthesis of ureas **29a** and **29b**, but also provided access to analogs with a variety of other substituents at the 7-position of 3-aminoindazole. Thus, demethylation of **26b** with BBr$_3$ followed by an *O*-alkylation of the produced phenol (**30**) led to various *O*-alkylated products (**31a**−**f**), from which ureas **34a**−**f** were readily synthesized (Scheme 4). Similarly, analogs with an aminomethyl-linked substituent at the 7-position of 3-aminoindazole such as **43a** and **43b** could be synthesized from bromide **39**, which was prepared via benzylic bromination of **26a** (Scheme 5).

Results and Discussion

Kinase enzymatic assays were performed utilizing the homogeneous time-resolved fluorescence (HTRF) protocol in the presence of a high concentration (1.0 mM) of ATP. Given that KDR plays a primary role in tumor angiogenesis, optimization of potency against KDR was emphasized in the SAR studies. The first compound of this series tested in the KDR assay was 3-aminoindazole aniline **9**. A moderate inhibitory activity (KDR IC$_{50}$ = 4790 nM) was measured for **9** (Table 1). This activity was very similar to that shown by the corresponding thienopyrimidine aniline **4** (KDR IC$_{50}$ = 4600 nM), indicating that the 3-aminoindazole nucleus indeed held the potential as a promising new template for RTK inhibitors. In fact, just as was seen in the thienopyrimidine series, the KDR potency improved remarkably when **9** was converted to an *N*,*N*′-diaryl urea. Phenyl urea **17a** (KDR IC$_{50}$ = 64 nM) was about 75-fold more potent than **9**. A further improved potency was observed for *m*-tolyl urea **17b** (KDR IC$_{50}$ = 3 nM). The substantially improved KDR potency shown by **17a** and **17b** was consistent with the proposed KDR binding model and clearly revealed the importance of the urea moiety for the KDR affinity. The importance of the urea link was further demonstrated by the significant loss of potency suffered by the amide analog (**13**) and the sulfonamide analog (**14**). Compound **14** was almost 88-fold less active against KDR than **17a**, while no apparent inhibitory activity was seen for **13**, even at a concentration of 12.5 *μ*M. Additionally, *N*,*N*′-diaryl ureas seemed to be optimal for KDR inhibition. Just as the phenyl analog (**17a**) and the *m*-tolyl analog (**17b**), 3-thiophene analog **17c** was also a very potent KDR inhibitor. Replacement of the urea terminal aromatic groups with a cyclopentyl or a cyclohexyl group still generated fairly potent KDR inhibitors

Scheme 2. Synthesis of N1-Substituted 3-Aminoindazole Ureas **22a−d**[a]

[a] Reagents and conditions: (i) RNHNH₂, *n*-BuOH, 110 °C, 80−90%; (ii) phthalic anhydride, dioxane, 110 °C, 31%; (iii) RBr, Na₂CO₃, DMF, 30−60%; (iv) NH₂NH₂·H₂O, EtOH, 0 °C → rt, 85−90%; (v) **10**, Pd(PPh₃)₄, Na₂CO₃, DME, H₂O, 90 °C, 45−70%; (vi) aryl isocyanate, DMF, 0 °C → rt, 30−70%; (vii) **16b**, Pd(PPh₃)₄, Na₂CO₃, DME, H₂O, 90 °C, 39%.

Scheme 3. Synthesis of 7-Substituted 3-Aminoindazole Ureas **29a−d**[a]

[a] Reagents and conditions: (i) LDA, THF, −78 °C, 1 h; then solid CO₂, −78 °C → rt, 60−80%; (ii) SOCl₂, reflux, 2 h or (COCl)₂, cat. DMF, rt; then concentrated aqueous NH₄OH, THF, 0 °C → rt, 90−98%; (iii) SOCl₂, DMF, 115 °C, 60−80%; (iv) NH₂NH₂·H₂O, *n*-BuOH, 110 °C, 80−90%; (v) **10**, Pd(PPh₃)₄, Na₂CO₃, toluene, EtOH, H₂O, 90 °C, or microwave, 140−160 °C, 20 min, 45−65%; (vi) *m*-tolyl isocyanate, CH₂Cl₂, 0 °C → rt, 35−70%.

Scheme 4. Synthesis of 7-Substituted 3-Aminoindazole Ureas **34a−f**[a]

[a] Reagents and conditions: (i) BBr₃, CH₂Cl₂, −78 °C, 77%; (ii) RBr, K₂CO₃; or ROH, DEAD, PPh₃, THF, 70−97%; (iii) NH₂NH₂·H₂O, *n*-BuOH, 110 °C, 50−70%; (iv) **10**, Pd(PPh₃)₄, DME, H₂O, 85 °C, or microwave, 140−160 °C, 15−20 min; (v) *m*-tolyl isocyanate, DMF, 0 °C → rt, 35−70%.

(**17d**: IC₅₀ = 153 nM and **17e**: IC₅₀ = 86 nM), but these aliphatic ureas had no obvious advantage over their aromatic analogs.

Further screening of these 3-aminoindazole ureas against other RTKs showed that they were also potent against other VEGFR kinases as well as the kinases of the PDGFR family. As the data in Table 1 show, these ureas were potent inhibitors of both FLT3 and cKIT. The SAR regarding cKIT was very similar to that displayed in KDR inhibition; an *N,N′*-diaryl urea moiety was also optimal for cKIT affinity. However, the binding affinity

for FLT3 appeared to be less sensitive to the nature of the urea terminal group. Potent activity against FLT3 was observed for both aromatic and aliphatic ureas. Given that mutational activation of FLT3 and cKIT are respectively implicated in AML and GIST, these compounds have potential as targeted therapeutics for these diseases.

Scheme 5. Synthesis of 7-Substituted 3-Aminoindazole Ureas **43a,b**[a]

a: R = 4-morpholinyl
b: R = 4-methylpiperazinyl

[a] Reagents and conditions: (i) NBS, $(PhCO_2)_2$, benzene, reflux, 46%; (ii) amine, DMF, rt, 90−98%; (iii) $NH_2NH_2 \cdot H_2O$, *n*-BuOH, 110 °C, 50−75%; (iv) **10**, $Pd(PPh_3)_4$, DME, H_2O, 85 °C, or microwave, 140−160 °C, 15−20 min; (v) *m*-tolyl isocyanate, DMF, 0 °C → rt, 40−60%.

Concluding that an *N,N'*-diaryl urea moiety at the C4-position of the aminoindazole nucleus was optimal for KDR inhibition, we then examined the substitution on the urea terminal phenyl group of **17a**. As the results in Table 2 show, incorporation of a fluoro or a methyl group on the phenyl group was tolerated at all three different positions (*meta-*, *ortho-*, and *para-*positions); however, consistent with the thienopyrimidine ureas,[22] the *meta*-substituted analogs (**17b** and **17g**) were the most potent in terms of KDR inhibitory activity. In fact, with an IC_{50} value of 3 nM, *m*-tolyl urea **17b** was one of the most potent KDR inhibitors of this series based on the enzymatic assay. Very potent KDR inhibitory activity was also achieved by introduction of an *m*-Et (**17k**: KDR IC_{50} = 6 nM), an *m*-Cl (**17l**: KDR IC_{50} = 8 nM), or an *m*-CF_3 (**17n**: KDR IC_{50} = 10 nM). The potency gain observed for these compounds bearing a *meta*-substituent in comparison to **17a** seems to be consistent with the modeling suggestion that an additional hydrophobic volume exists near the *meta*-position. Substitution with an *m*-Br or *m*-OH is also tolerated. Introduction of an additional fluoro group on the *m*-tolyl ring of **17b** and the *p*-tolyl ring of **17j** had no impact on the KDR affinity, but as discussed later, these analogs (**17p**, **17q**, and **17r**) exhibited improved in vivo properties (see the data in Table 5 and the related discussion). Incorporation of an additional fluoro group at the *meta*-position to the CF_3 group on the phenyl in **17n** (KDR IC_{50} = 10 nM), on the other hand, caused a 9-fold reduction in KDR affinity (**17s**: KDR IC_{50} = 90 nM).

The SAR at the endocyclic indazole NH was also explored. The modeling suggested that there was no direct hydrogen-bonding interaction between the NH and the KDR protein and, consequently, elaboration at the NH position might be tolerated. Indeed, *N*-methylation of the NH in **17b** only caused a slight drop in KDR potency. Compound **22a** was still a very potent

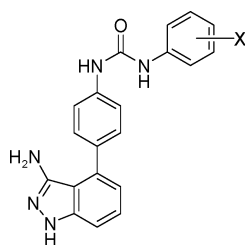**Table 1.** RTK Inhibitory Activity of C4-Substituted Aminoindazoles

Compd	R	KDR IC_{50}, nM[a]	FLT3 IC_{50}, nM[a]	cKIT IC_{50}, nM[a]
9	NH_2	4,790	43	7,360
13	HN–C(=O)–phenyl	>12,500	694	>12,500
14	HN–S(=O)$_2$–phenyl	4,620	--	11,200
17a	HN–C(=O)–NH–phenyl	64	54	44
17b	HN–C(=O)–NH–(3-CH_3-phenyl)	3	12	17
17c	HN–C(=O)–NH–thienyl	15	5	42
17d	HN–C(=O)–NH–cyclopentyl	153	39	850
17e	HN–C(=O)–cyclohexyl	86	13	152

[a] Each IC_{50} determination was performed with seven concentrations, and each assay point was determined in duplicate.

KDR inhibitor, exhibiting an IC_{50} value of 11 nM (Table 3). However, significant loss of KDR potency was observed for all other groups examined (**22b−d**). The unfavorable steric interaction imposed by these larger groups might be responsible for the reduction in potency.
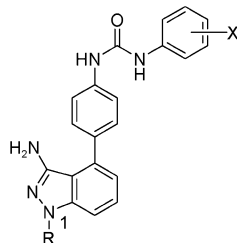
Based on the proposed binding model, a substituent at the 7-position of the 3-aminoindazole nucleus should project toward solvent and, thus, chemical elaborations aimed at modulating physiochemical properties at this position should be tolerated. Indeed, the SAR of this position was consistent with this prediction (Table 4). Substituents such as Me, MeO, F, and Br (**29a−d**) as well as various polar groups that were attached to the position via a three-atom ether link (CH_2CH_2O; **34a−f**) were well tolerated. Nonetheless, when the link was shortened to a methylene unit, reduced RTK inhibitory activity was observed (**43a**: KDR IC_{50} = 390 nM; **43b**: KDR IC_{50} = 1200 nM). Compounds **43a** and **43b** were not only poor KDR inhibitors, but also weak against FLT3 and cKIT. In these cases, the 4-methylpiperazino and morpholino groups in close proximity to the 3-aminoindazole nucleus might disrupt the interaction between the 3-aminoindazole core and the hinge region of the kinases.

The proposed hydrogen-bonding interactions between the 3-aminoindazole moiety and the two amino acid residues (Glu 917 and Cys 919) of the KDR hinge region should be vital to the binding affinity of these inhibitors. Interrupting these interactions would predictably have a large negative impact on potency. Indeed, this was clearly demonstrated by the significant

Table 2. Substitutions at the Terminal Phenyl of the *N,N'*-Diaryl Ureas

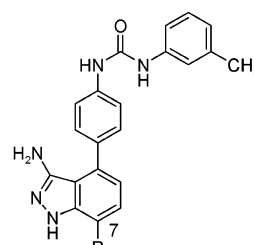| cmpd	X	KDR IC$_{50}^{a}$ (nM)	FLT3 IC$_{50}^{a}$ (nM)	cKIT IC$_{50}^{a}$ (nM)
17a	H	64	54	44
17f	*o*-F	82	157	34
17g	*m*-F	23	25	15
17h	*p*-F	67	26	20
17i	*o*-Me	87	3	86
17b	*m*-Me	3	4	20
17j	*p*-Me	12	2	17
17k	*m*-Et	6	55	42
17l	*m*-Cl	8	3	13
17m	*m*-Br	36	106	69
17n	*m*-CF$_3$	10	10	41
17o	*m*-OH	55	26	48
17p	2-F-5-Me	4	5	16
17q	4-F-3-Me	4	7	10
17r	3-F-4-Me	36	47	42
17s	2-F-5-CF$_3$	90	270	150

^{a} Each IC$_{50}$ determination was performed with seven concentrations, and each assay point was determined in duplicate.

Table 3. N1-Substitution of 3-Aminoindazoles

Compd	R	X	KDR IC$_{50}$, nM^a	FLT3 IC$_{50}$, nM^a
22a	Me	Me	11	8
22b	CH$_2$CH$_2$OH	Me	600	270
22c	CH$_2$CH$_2$-morpholine	Me	1,300	860
22d	CH$_2$CH$_2$OMe	2-F-5-Me	3,090	480

^{a} Each IC$_{50}$ determination was performed with seven concentrations, and each assay point was determined in duplicate.

loss in KDR potency observed for both **44** and **45** (>1000-fold and 290-fold, respectively; Figure 5) in comparison to **22a** (KDR IC$_{50}$ = 11 nM). It appeared that the added groups at the 3-amino residue in **44** and **45** not only affected the hydrogen bonding interaction between the amino group and the Glu 917 of KDR, but also the one between the indazole ring nitrogen (N2) and Cys 919 residue, because indazole urea **46**, which does not possess a 3-amino group, was still fairly potent against KDR. With an IC$_{50}$ value of 465 nM, **46** was only about 42-fold less

Table 4. Substitutions at the 7-Position of 3-Aminoindazoles

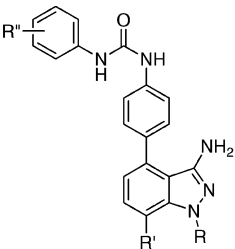| Compd	R	KDR IC$_{50}$, nM^a	FLT3 IC$_{50}$, nM^a	cKIT IC$_{50}$, nM^a
17b	H	3	17	12
29a	Me	3		10
29b	MeO	26	29	28
29c	F	5	14	5
29d	Br	10	13	39
34a	O(CH$_2$)$_2$NMe$_2$	38	73	65
34b	O(CH$_2$)$_2$NEt$_2$	35	60	61
34c	O(CH$_2$)$_2$N-pyrrolidine	31	120	26
34d	O(CH$_2$)$_2$N-morpholine	21	24	50
34e	O(CH$_2$)$_2$N-pyrrolidinone	25	15	53
34f	O(CH$_2$)$_2$OMe	21	34	32
43a	CH$_2$N-morpholine	390	450	400
43b	CH$_2$N-methylpiperazine	1,200	215	290

^{a} Each IC$_{50}$ determination was performed with seven concentrations, and each assay point was determined in duplicate.
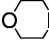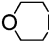
potent than its 3-amino analog **22a**. Interestingly, an even more potent activity was recorded for indazole urea **47** (KDR IC$_{50}$ = 18 nM), which was only 6-fold less potent than **17b**. At this point, it is not clear whether the hydrogen-bonding interaction between the indazole ring nitrogen and Cys 919 of KDR became more optimal in the absence of substituents at both indazole N1- and C3-positions in **47** or whether the indazole ring NH also contributes to the potency.

Based on the results of the KDR enzymatic assay, selected 3-aminoindazole ureas were further characterized as indicated in Table 5. The potent inhibition of these inhibitors against KDR was generally well reflected at the cellular level. As the results in Table 5 show, these compounds potently inhibited VEGF-induced KDR phosphorylation in 3T3-murine fibroblast cells engineered to express human KDR, mostly exhibiting IC$_{50}$ values in the low double-digit nanomolar range. It is noteworthy that the incorporation of various water-solubilizing groups at the 7-position of the indazole yielded very comparable cellular KDR activity relative to the KDR enzymatic potency (lower portion of Table 5).
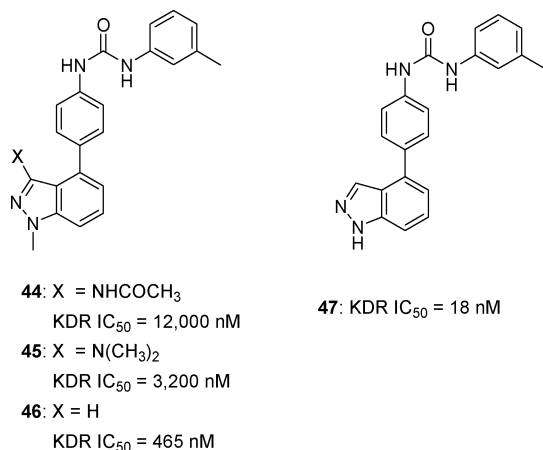
To evaluate the in vivo activity, compounds with potent cellular activity were first screened in an estradiol-induced mouse uterine edema (UE) model.[22] This functional assay served as a useful tool for a rapid and preliminary evaluation of KDR inhibitors' oral activity. Among the three methyl-substituted 3-aminoindazole ureas (**17b**, **17i**, and **17j**), only the *meta*-methyl

Table 5. In Vitro and In Vivo Properties of Selected 3-Aminoindazole Ureas

Compd	R	R'	R"	KDR[a] IC$_{50}$, nM	KDR (cell)[b] IC$_{50}$, nM	UE[c] ED$_{50}$, mg/kg	HT1080[e]	Mouse PK AUC[g] (μM•h)	F (%)
17b	H	H	*m*-Me	3	13	4		6.5	38
17i	H	H	*o*-Me	87	80	0% @ 10[d]			
17j	H	H	*p*-Me	12	12	0% @ 10[d]			
17l	H	H	*m*-Cl	8	28	3.5	72% @ 10[f]	15	50
17n	H	H	*m*-CF$_3$	10	32	4	64% @ 10[f]		
17p	H	H	2-F-5-Me	4	4	0.5	69% @ 10[f]	24.5	100
17q	H	H	4-F-3-Me	4	9	105% @ 10[d]		10.9	66
17r	H	H	3-F-4-Me	36	48	49% @ 10[d]			
17s	H	H	2-F-5-CF$_3$	90	151	73% @ 10[d]			
22a	Me	H	*m*-Me	11	23	3	69% @ 10[f]	19.8	89
34f	H	MeO(CH$_2$)$_2$O	*m*-Me	21	15	57% @ 10[d]			
35	H	MeO(CH$_2$)$_2$O	*m*-Cl	13	16	35% @ 10[d]			
36	H	MeO(CH$_2$)$_2$O	2-F-5-Me	21	33	9% @ 10[d]			
34a	H	Me$_2$N(CH$_2$)$_2$O	*m*-Me	35	12	8% @ 10[d]			
37	H	Et$_2$N(CH$_2$)$_2$O	2-F-5-Me	74	15	56% @ 10[d]			
34d	H	O⏝N(CH$_3$)$_2$O	*m*-CH$_3$	21	56	52% @ 10[d]		1.0	20
38	H	O⏝N(CH$_3$)$_2$O	2-F-5-Me	62	37	76% @ 10[d]	59% @ 30[f]	2.5	25

[a] Each IC$_{50}$ determination was performed with seven concentrations, and each assay point was determined in duplicate. [b] Activity against VEGF-induced KDR phosphorylation in 3T3-murine fibroblast cells. Each cellular IC$_{50}$ determination was performed with five concentrations, and each assay point was determined in duplicate. [c] Dosed orally in balb/c female mice. [d] Percent inhibition in mg/kg. [e] Dosed orally twice a day in SCID-beige mice. [f] Tumor percent inhibition as the total daily dose (mg/kg). [g] Dosed orally at 10 mg/kg in CD-1 mice.

44: X = NHCOCH$_3$
KDR IC$_{50}$ = 12,000 nM

45: X = N(CH$_3$)$_2$
KDR IC$_{50}$ = 3,200 nM

46: X = H
KDR IC$_{50}$ = 465 nM

47: KDR IC$_{50}$ = 18 nM

Figure 5. Indazole ureas **44−47** and their activity against KDR.

analog **17b** showed potent oral activity in the UE model at an oral dose of 10 mg/kg. Although the *para*-methyl analog **17j** displayed a very similar KDR cellular activity to that shown by **17b**, it produced no inhibition of the edema at the same dose. It appeared that substitution with a small lipophilic group on the *meta*-position of the urea terminal phenyl group not only gave the best KDR enzymatic potency (cf. data in Table 2), but also delivered potent in vivo activity. This was further demonstrated by the efficacy of **17l**, **17n**, and **22a** in the UE model, with each exhibiting an ED$_{50}$ value equal to or less than 4 mg/kg. Possessing a 2-fluoro-5-methylphenyl group, compound **17p** was extremely potent (ED$_{50}$ = 0.5 mg/kg) and compared favorably in this model to both **5** and **2**, which displayed an ED$_{50}$ value of 5 mg/kg and 11 mg/kg, respectively. As was mentioned before, the fluoro group in **17p** had no impact on the KDR enzymatic potency in comparison to **17b**; however, **17p** showed a significantly enhanced UE potency, which is consistent with its much improved mouse oral plasma exposure (AUC at an oral dose of 10 mg/kg: 24.5 μM·h for **17p** vs 6.5 μM·h for **17b**). Incorporation of a fluoro group on the urea terminal aryl group also led to an improved mouse oral pharmacokinetic (PK) profile for **17q** and an enhanced UE

Table 6. Kinase Inhibition Profile of **17p**

kinase	IC_{50}^{a} (nM)	kinase	IC_{50}^{a} (nM)
KDR	4	RET	1,900
FLT1	3	FGFR	12,500
FLT4	190	SRC	50,000
PDGFRβ	66	IGFR	50,000
CSF1R	3	LCK	50,000
KIT	14	FGR	50,000
FLT3	4	AKT^{b}	50,000
TIE2	170	CDC2^{b}	9,800

^{a} Each IC_{50} determination was performed with seven concentrations, and each assay point was determined in duplicate. ^{b} IC_{50} values were determined at an ATP concentration of 5−10 μmol/L.

Table 7. PK Profile of **17p**

	IV			PO	
species	$t_{1/2}$ (h)	V_{d} (L/kg)	Cl (mL/min·kg)	AUC (μg·h/mL)	F (%)
rat^{a}	3.6	1.1	3.3	6.8	27.0
monkey^{b}	3.1	2.2	8.2	0.6	10.6
dog^{b}	2.0	1.2	7.2	1.5	47.0

^{a} Dosed at 5 mg/kg both intravenously and orally. ^{b} Dosed at 2.5 mg/kg both intravenously and orally.

activity for **17r** when compared to **17b** and **17j**, respectively. Compounds with a water-solubilizing group at the indazole C7-position generally appeared less potent in the edema model than their unsubstituted analogs, in spite of their comparable KDR cellular activity. The limited mouse oral exposure of **34d** and **38** provided one explanation for their poor activity in the edema model.

Select compounds with potent oral activity in the UE model were then evaluated in an HT1080 fibrosarcoma xenograft tumor growth model for their antitumor activity. Consistent with their potent activity in the UE model and good oral exposure profiles, compounds **17l**, **17p**, and **22a** showed significant tumor growth inhibition (around 70%) when dosed orally at 10 mg/kg daily whereas **38** was less efficacious even at a higher dose (30 mg/kg). Compound **17p** was further investigated in a number of other preclinical tumor growth models and significant efficacy was also observed. For example, it displayed 87% inhibition of tumor growth in DLD-1 colon carcinoma and 76% inhibition in MX-1 breast carcinoma, respectively, at a daily oral dose of 12.5 mg/kg.[25]

The significant antitumor efficacy of **17p** might be ascribed to its potent multitargeted kinase inhibition. As Table 6 shows, it potently inhibited all the members of the VEGFR and PDGFR families, but was generally highly selective over other structurally nonrelated tyrosine kinases, such as SRC and IGFR, as well as a number of selected serine/threonine kinases (e.g., AKT, CDC2). As a potent FLT3 inhibitor, **17p** may be promising in treating AMLs with overactivated FLT3. This was demonstrated by its impressive efficacy in a mouse flank xenograft model of MV-4−11 leukemia cells, in which FLT3 is constitutively activated by an ITD mutation. Rapid tumor regression was achieved when **17p** was given twice a day orally at a daily dose ≥1.5 mg/kg.[25]

The efficacy exhibited by **17p** in tumor growth inhibition warranted its further investigation. Although this compound is physically characterized by high lipophilicity (logD = 4.2 at pH 7.4) and low aqueous solubility (27 ng/mL at pH 7 at room temperature), it displayed favorable PK profiles across the species. Table 7 shows the PK data obtained from the evaluation of **17p** in Sprague−Dawley rat, Beagle dog, and cynomolgus monkey. In these species, **17p** exhibited moderate volumes of distribution (1.0−2.2 L/kg) and low plasma clearance (3.3−

8.2 mL/min·kg) following intravenous (IV) dosing. Its plasma IV half-lives ranged from 2.0 h in dog to 3.6 h in rat, while oral bioavailability ranged from 10 to 47%.

Consistent with its lipophilic character, **17p** displayed extensive plasma protein binding with 96.8% in monkey, 98.2% in mouse, and 99.1% in rat. In human plasma, the value is 99.0%. Compound **17p** did not show significant activity against the I_{kr} potassium channel hERG (human ether-a-go-go-related gene), as measured in a patch clamp assay. Only 5.9% blockage of hERG current in transfected HEK 293 cells was observed at a concentration of 0.35 μM. Additionally, no effect on the action potential duration of canine Purkinje fibers was measured with **17p** at a concentration of 5.45 μM using standard in vitro microelectrode techniques.

In vitro metabolism studies of **17p** showed that its metabolic turnover was low in mouse, dog, monkey, and human hepatocytes. About 91−92% of the parent drug remained after 6 h incubation. A number of major metabolites in human hepatocytes were identified, which include oxidation products **48** and **49**, *N*-glucoronidation product **50**, and oxidation/glucoronidation product **51** (Figure 6). While the exact hydroxylation positions in **48** and **51** are not clear yet, the structures of **49** and **50** have been confirmed. Compound **49** was tested in the KDR enzymatic assay and showed no significant inhibition of KDR (IC_{50} = 6580 nM).

With its potent activity against VEGF and PDGF receptor tyrosine kinases, good oral PK profile across the species, and efficacious antitumor activity in the multiple preclinical models, **17p** was advanced into clinical evaluation.

Conclusion

Potent multitargeted RTK inhibitors with manageable adverse effects hold great promise as anticancer agents. Through a structure-based approach, we identified 3-aminoindazole as a novel kinase inhibitor template, which mimicked the adenine of ATP interacting with the kinase hinge region through a pair of hydrogen-bonding interactions. Incorporation of an *N,N′*-diaryl urea moiety at the 4-position of the indazole ring afforded a series of compounds that potently inhibited VEGFR and PDGFR kinases. A KDR homology model suggested that these compounds bind to the ATP-binding site of an inactive KDR conformation, with the urea portion interacting with the distal hydrophobic pocket. By optimizing the substituents at both the urea terminal phenyl ring and the 7-position of the 3-aminoindazole, a series of compounds with potent enzymatic and cellular activity were obtained. A number of these compounds possessed potent oral activity in the mouse UE model. In particular, compound **17p** was extremely potent, with an ED_{50} value of 0.5 mg/kg. Further evaluation of **17p** showed that it displayed good PK profiles in different species and significantly inhibited tumor growth in a number of preclinical animal models. Based on its overall in vitro and in vivo profile, **17p** was chosen for clinical evaluation.

Experimental Section

Chemistry. ^{1}H NMR spectra were recorded on a 300 MHz spectrometer (GE QE300) if not otherwise indicated, and chemical shifts are reported in parts per million (ppm, δ) relative to tetramethylsilane as an internal standard. Mass spectra were obtained on a Finnigan MAT SSQ700 instrument. Elemental analysis (C, H, N) was performed by Robertson Microlit Laboratories, Inc., Madison, NJ, and the results indicated by elemental symbols are within ±0.4% of theoretical values. Silica gel 60 (E. Merck, 230−400 mesh) was used for flash column chromatography. Preparative HPLC was performed on a Waters Symmetry C8
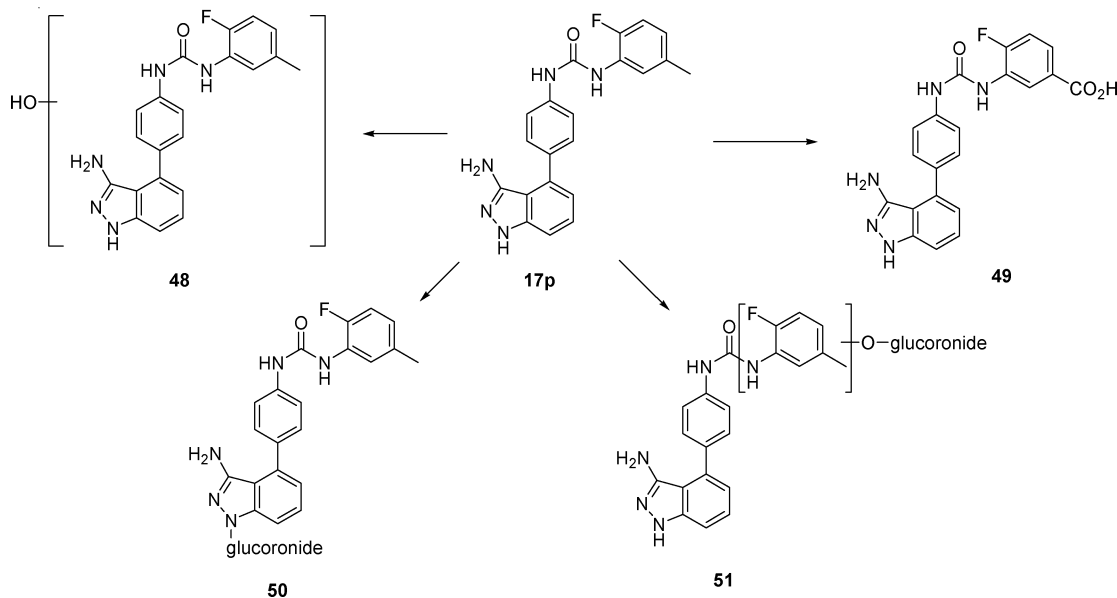
Figure 6. In vitro metabolic pathways of **17p**.

column (25 mm × 100 mm, 7 μm particle size) using a gradient of 10−100% acetonitrile in water containing 0.1% trifluoroacetic acid (TFA) over 8 min (10 min run time) at a flow rate of 40 mL/ min.

4-Iodo-1*H*-indazol-3-amine (8). A mixture of 2-fluoro-6-iodobenzonitrile (2.0 g, 8.1 mmol) and hydrazine monohydrate (4 mL) in *n*-butanol (40 mL) was stirred at 105−110 °C for 5 h and then cooled to room temperature, poured into water, and extracted twice with ethyl acetate. The combined extracts were washed with water and brine, dried (MgSO$_4$), filtered, and concentrated to provide the title compound (1.88 g, 90%). ^{1}H NMR (DMSO-d_6) δ 5.04 (s, 2H), 6.93 (dd, $J = 8.14$, 7.12 Hz, 1H), 7.29 (d, $J = 8.48$ Hz, 1H), 7.34 (d, $J = 7.12$ Hz, 1H), 11.78 (s, 1H); MS (ESI) m/z 260 (M + H)$^+$.

4-(4-Aminophenyl)-1*H*-indazol-3-ylamine (9). A mixture of **8** (467 mg, 1.81 mmol), 4-(4,4,5,5-tetramethyl-1,3,2-dioxaborolan-2-yl)aniline (**10**; 435 mg, 1.99 mmol), Na$_2$CO$_3$ (526 mg, 4.96 mmol), and Pd(PPh$_3$)$_4$ (104 mg, 0.09 mmol) in toluene (20 mL), ethanol (20 mL), and water (10 mL) was heated at 90 °C for 16 h under a nitrogen atmosphere. After being cooled to room temperature, the mixture was partitioned between ethyl acetate and water. The aqueous layer was extracted with ethyl acetate twice, and the combined organic layers were washed with brine, dried (MgSO$_4$), filtered, and concentrated. The crude product was purified by flash column chromatography on silica gel with 3−8% methanol in dichloromethane to give the title compound (243 mg, 60%). ^{1}H NMR (DMSO-d_6) δ 4.34 (s, 2H), 5.25 (s, 2H), 6.62−6.74 (m, 3H), 7.06−7.29 (m, 4H), 11.59 (s, 1H); MS (ESI) m/z 225 (M + H)$^+$. Anal. (C$_{13}$H$_{12}$N$_4$·0.3H$_2$O·0.1EtOAc) C, H, N.

N-[4-(4,4,5,5-Tetramethyl-[1,3,2]dioxaborolan-2-yl)phenyl]-benzamide (11). To a solution of 4-(4,4,5,5-tetramethyl-1,3,2-dioxaborolan-2-yl)aniline (**10**; 500 mg, 2.28 mmol) in methylene chloride (10 mL) cooled with an ice−water bath was added triethylamine (477 μL, 3.42 mmol) and benzoyl chloride (248 μL, 2.28 mmol). The mixture was stirred overnight, washed with water, dried (MgSO$_4$), filtered, and concentrated to give the title compound as a white solid (700 mg, 95%). ^{1}H NMR (DMSO-d_6) δ 1.30 (s, 12H), 7.50−7.62 (m, 3H), 7.66 (d, $J = 8.48$ Hz, 2H), 7.82 (d, $J = 8.48$ Hz, 2H), 7.93−7.98 (m, 2H), 10.34 (s, 1H); MS (ESI) m/z 324 (M + H)$^+$.

N-[4-(3-Amino-1*H*-indazol-4-yl)phenyl]benzamide (13). A mixture of **8** (100 mg, 0.31 mmol), **11** (120 mg, 0.37 mmol), Na$_2$CO$_3$ (82 mg, 0.77 mmol), and Pd(dppf)Cl$_2$·CH$_2$Cl$_2$ (13 mg, 0.015 mmol) in 1,2-dimethoxyethane (DME; 3 mL) and water (1 mL) was purged with bubbling nitrogen for 2 min and then heated at 150 °C for 20 min in a Smith Synthesizer microwave oven (300 W). After being

cooled to room temperature, the mixture was partitioned between ethyl acetate and water. The aqueous layer was extracted twice with ethyl acetate, and the combined organic layers were washed with brine, dried (MgSO$_4$), filtered, and concentrated. The crude product was purified by flash column chromatography on silica gel with ethyl acetate to give the title compound (60 mg, 59%). ^{1}H NMR (DMSO-d_6) δ 4.32 (s, 2H), 6.81 (dd, $J = 5.09$, 2.71 Hz, 1H), 7.24−7.33 (m, 2H), 7.47 (d, $J = 8.48$ Hz, 2H), 7.51−7.64 (m, 3 H), 7.93 (d, $J = 8.82$ Hz, 2H), 7.96−8.01 (m, 2H), 10.39 (s, 1H), 11.72 (s, 1H); MS (ESI) m/z 329 (M + H)$^+$. Anal. (C$_{20}$H$_{16}$N$_4$O·0.3H$_2$O) C, H, N.

N-[4-(3-Amino-1*H*-indazol-4-yl)phenyl]benzenesulfonamide (14). Compound **14** was prepared from **8** using the same procedure as for **13**. ^{1}H NMR (DMSO-d_6) δ 4.19 (s, 2H), 6.71 (dd, $J = 4.58$, 3.22 Hz, 1H), 7.16−7.26 (m, 4H), 7.29−7.36 (m, 2H), 7.52−7.67 (m, 3H), 7.79 (d, $J = 6.78$ Hz, 2H), 10.45 (s, 1H), 11.72 (s, 1H); MS (ESI) m/z 365 (M + H)$^+$.

General Procedure for the Synthesis of Urea Boronates 16a−s. A solution of 4-(4,4,5,5-tetramethyl-1,3,2-dioxaborolan-2-yl)-aniline (**10**; 500 mg, 2.28 mmol) in methylene chloride (10 mL) was treated with the corresponding isocyanate (2.28 mmol) and stirred at room temperature overnight. The formed solid material was collected by filtration to provide the desired urea boronates. In the cases in which only little or no precipitate was formed after the reaction, the reaction mixture was concentrated and the product was precipitated out by adding hexanes to the concentrated solution.

N-Phenyl-N′-[4-(4,4,5,5-tetramethyl-1,3,2-dioxaborolan-2-yl)-phenyl]urea (16a). ^{1}H NMR (500 MHz, DMSO-d_6) δ 1.28 (s, 12H), 6.98 (t, $J = 7.32$ Hz, 1H), 7.26−7.31 (m, 2H), 7.46 (t, $J = 8.24$ Hz, 4H), 7.59 (d, $J = 8.24$ Hz, 2H), 8.70 (s, 1H), 8.81 (s, 1H); MS (ESI) m/z 339 (M + H)$^+$.

Spectral data of urea boronates **16b−s** are given in the Supporting Information.

General Procedures for the Synthesis of 3-Aminoindazole Ureas 17a−s. Method A: A mixture of **8** (60 mg, 0.24 mmol), urea boronate (0.29 mmol), and Na$_2$CO$_3$ (64 mg, 0.60 mmol) under a nitrogen atmosphere was treated with DME (9 mL), water (3 mL), and Pd(dppf)Cl$_2$·CH$_2$Cl$_2$ (10 mg, 0.012 mmol). The mixture was purged with bubbling nitrogen for 2 min, and then stirred at 85 °C for 16 h, cooled to room temperature, and partitioned between ethyl acetate and water. The aqueous layer was extracted with ethyl acetate twice, and the combined organic layers were washed with brine, dried (MgSO$_4$), filtered, and concentrated. The crude product was purified either by flash column chromatography on silica gel eluting first with ethyl acetate and then 4−8% methanol in dichloromethane or by preparative HPLC.

Method B: A mixture of **8** (60 mg, 0.24 mmol), urea boronate (0.29 mmol), Na$_2$CO$_3$ (64 mg, 0.60 mmol), and Pd(dppf)Cl$_2$·CH$_2$-Cl$_2$ (10 mg, 0.012 mmol) in DME (3 mL) and water (1 mL) in a microwave vial was degassed by bubbling through nitrogen for 1−2 min. The reaction vial was then capped and heated at 140−160 °C under stirring for 15−20 min in a Smith Synthesizer microwave oven (300 W). The reaction mixture was worked up and purified as in Method A.

N-[4-(3-Amino-1H-indazol-4-yl)phenyl]-N′-phenylurea (17a). ^{1}H NMR (DMSO-d_6) δ 4.33 (s, 2H), 6.78 (dd, J = 5.42, 2.37 Hz, 1H), 6.98 (t, J = 7.29 Hz, 1H), 7.28 (m, 4H), 7.39 (d, J = 8.81 Hz, 2H), 7.48 (d, J = 7.46 Hz, 2H), 7.59 (d, J = 8.82 Hz, 2H), 8.72 (s, 1H), 8.81 (s, 1H), 11.70 (s, 1H); MS (ESI) m/z 344 (M + H)$^+$. Anal. (C$_{20}$H$_{17}$N$_5$O·0.5EtOAc) C, H, N.

N-[4-(3-Amino-1H-indazol-4-yl)phenyl]-N′-(3-methylphenyl)-urea (17b). ^{1}H NMR (DMSO-d_6) δ 2.29 (s, 3H), 4.33 (s, 2H), 6.76−6.83 (m, 2H), 7.17 (t, J = 7.80 Hz, 1H), 7.23−7.28 (m, 3H), 7.32 (s, 1H), 7.39 (d, J = 8.48 Hz, 2H), 7.59 (d, J = 8.48 Hz, 2H), 8.64 (s, 1H), 8.79 (s, 1H), 11.70 (s, 1H); MS (ESI) m/z 358 (M + H)$^+$. Anal. (C$_{21}$H$_{19}$N$_5$O·0.8H$_2$O) C, H, N.

N-[4-(3-Amino-1H-indazol-4-yl)-phenyl]-N′-thiophen-3-yl-urea (17c). ^{1}H NMR (DMSO-d_6) δ 4.33 (s, 2H), 6.78 (dd, J = 5.59, 2.20 Hz, 1H), 7.07 (dd, J = 5.09, 1.36 Hz, 1H), 7.24−7.28 (m, 2H), 7.29−7.33 (m, 1H), 7.39 (d, J = 8.48 Hz, 2H), 7.45 (dd, J = 5.09, 3.39 Hz, 1H), 7.59 (d, J = 8.48 Hz, 2H), 8.78 (s, 1H), 8.99 (s, 1H), 11.70 (s, 1H); MS (ESI) m/z 350 (M + H)$^+$. Anal. (C$_{18}$H$_{15}$N$_5$OS·0.1C$_6$H$_{14}$·0.3H$_2$O) C, H, N.

N-[4-(3-Amino-1H-indazol-4-yl)-phenyl]-N′-cyclopentylurea (17d). ^{1}H NMR (DMSO-d_6) δ 1.31−1.45 (m, 2H), 1.47−1.71 (m, 4H), 1.77−1.93 (m, 2H), 3.89−4.00 (m, 1H), 4.31 (s, 2H), 6.21 (d, J = 7.12 Hz, 1H), 6.75 (dd, J = 5.59, 2.20 Hz, 1H), 7.22−7.27 (m, 2H), 7.32 (d, J = 8.48 Hz, 2H), 7.50 (d, J = 8.48 Hz, 2H), 8.39 (s, 1H), 11.68 (s, 1H); MS (ESI) m/z 336 (M + H)$^+$.

N-[4-(3-Amino-1H-indazol-4-yl)-phenyl]-N′-cyclohexylurea (17e). ^{1}H NMR (DMSO-d_6) δ 1.09−1.41 (m, 5H), 1.48−1.60 (m, 1H), 1.60−1.73 (m, 2H), 1.77−1.89 (m, 2H), 3.42−3.56 (m, 1H), 4.30 (s, 2H), 6.12 (d, J = 7.80 Hz, 1H), 6.75 (dd, J = 5.59, 2.20 Hz, 1H), 7.19−7.26 (m, 2H), 7.32 (d, J = 8.82 Hz, 2H), 7.50 (d, J = 8.82 Hz, 2H), 8.43 (s, 1H), 11.67 (s, 1H); MS (ESI) m/z 350 (M + H)$^+$. Anal. (C$_{20}$H$_{23}$N$_5$O·0.2H$_2$O·0.3EtOAc) C, H, N.

N-[4-(3-Amino-1H-indazol-4-yl)phenyl]-N′-(2-fluorophenyl)-urea (17f). ^{1}H NMR (DMSO-d_6) δ 4.33 (s, 2H), 6.79 (dd, J = 5.42, 2.71 Hz, 1H), 6.97−7.06 (m, 1H), 7.16 (t, J = 7.63 Hz, 1H), 7.22−7.30 (m, 3H), 7.41 (d, J = 8.48 Hz, 2H), 7.60 (d, J = 8.48 Hz, 2H), 8.18 (m, 1H), 8.61 (d, J = 2.37 Hz, 1H), 9.22 (s, 1H), 11.71 (s, 1H); MS (ESI) m/z 362 (M + H)$^+$. Anal. (C$_{20}$H$_{16}$-FN$_5$O·0.7CH$_2$Cl$_2$·0.1EtOAc) C, H, N.

N-[4-(3-Amino-1H-indazol-4-yl)phenyl]-N′-(3-fluorophenyl)-urea (17g). ^{1}H NMR (DMSO-d_6) δ 4.33 (s, 2H), 6.75−6.83 (m, 2H), 7.15 (m, 1H), 7.23−7.36 (m, 3H), 7.40 (d, J = 8.48 Hz, 2H), 7.52 (m, 1H), 7.59 (d, J = 8.48 Hz, 2H), 8.89 (s, 1H), 8.97 (s, 1H), 11.71 (s, 1H); MS (ESI) m/z 362 (M + H)$^+$. Anal. (C$_{20}$H$_{16}$-FN$_5$O·0.2C$_6$H$_{14}$·0.2EtOAc) C, H, N.

N-[4-(3-Amino-1H-indazol-4-yl)phenyl]-N′-(4-fluorophenyl)-urea (17h). ^{1}H NMR (DMSO-d_6) δ 4.33 (s, 2H), 6.78 (dd, J = 5.43, 2.37 Hz, 1H), 7.13 (t, J = 8.99 Hz, 2H), 7.22−7.29 (m, 2H), 7.39 (d, J = 8.48 Hz, 2H), 7.49 (m, 2H), 7.59 (d, J = 8.82 Hz, 2H), 8.80 (d, J = 15.60 Hz, 2H), 11.70 (s, 1H); MS (ESI) m/z 362 (M + H)$^+$. Anal. (C$_{20}$H$_{16}$FN$_5$O·0.7H$_2$O) C, H, N.

N-[4-(3-Amino-1H-indazol-4-yl)phenyl]-N′-(2-methylphenyl)-urea (17i). ^{1}H NMR (DMSO-d_6) δ 2.21−2.33 (m, 3H), 4.33 (s, 2H), 6.78 (dd, J = 5.76, 2.37 Hz, 1H), 6.96 (t, J = 7.46 Hz, 1H), 7.12−7.21 (m, 2H), 7.22−7.32 (m, 2H), 7.39 (d, J = 8.82 Hz, 2H), 7.60 (d, J = 8.82 Hz, 2H), 7.84 (d, J = 7.12 Hz, 1H), 7.97 (s, 1H), 9.15 (s, 1H), 11.69 (s, 1H); MS (ESI) m/z 358 (M + H)$^+$. Anal. (C$_{21}$H$_{19}$N$_5$O·0.6H$_2$O) C, H, N.

N-[4-(3-Amino-1H-indazol-4-yl)-phenyl]-N′-(4-methylphenyl)-urea (17j). ^{1}H NMR (DMSO-d_6) δ 2.25 (s, 3H), 4.32 (s, 2H), 6.78 (dd, J = 5.43, 2.37 Hz, 1H), 7.10 (d, J = 8.14 Hz, 2H), 7.21−7.31 (m, 2H), 7.33−7.43 (m, 4H), 7.58 (d, J = 8.82 Hz, 2H), 8.60 (s,

1H), 8.75 (s, 1H), 11.69 (s, 1H); MS (ESI) m/z 358 (M + H)$^+$. Anal. (C$_{21}$H$_{19}$N$_5$O·0.4H$_2$O) C, H, N.

N-(4-(3-Amino-1H-indazol-4-yl)phenyl)-N′-(3-ethylphenyl)-urea (17k). ^{1}H NMR (DMSO-d_6) δ 1.19 (t, J = 7.63 Hz, 3H), 2.58 (q, J = 7.68 Hz, 2H), 6.80−6.89 (m, 2H), 7.19 (t, J = 7.80 Hz, 1H), 7.25−7.45 (m, 6H), 7.60 (d, J = 8.81 Hz, 2H), 8.70 (s, 1H), 8.85 (s, 1H); MS (ESI) m/z 372 (M + H)$^+$. Anal. (C$_{22}$H$_{21}$N$_5$O·0.8CF$_3$CO$_2$H·0.2H$_2$O) C, H, N.

N-[4-(3-Amino-1H-indazol-4-yl)phenyl]-N′-(3-chlorophenyl)-urea (17l). ^{1}H NMR (DMSO-d_6) δ 6.89 (dd, J = 6.44, 1.70 Hz, 1H), 7.03 (m, 1H), 7.28−7.38 (m, 4H), 7.42 (d, J = 8.81 Hz, 2H), 7.61 (d, J = 8.82 Hz, 2H), 7.74 (m, 1H), 9.00 (s, 1H), 9.03 (s, 1H); MS (ESI) m/z 378 (M + H)$^+$. Anal. (C$_{20}$H$_{16}$ClN$_5$O·1.0CF$_3$-CO$_2$H·0.5H$_2$O) C, H, N.

N-[4-(3-Amino-1H-indazol-4-yl)phenyl]-N′-(3-bromophenyl)-urea (17m). ^{1}H NMR (DMSO-d_6) δ 6.87 (dd, J = 6.10, 1.70 Hz, 1H), 7.13−7.18 (m, 1H), 7.25 (t, J = 7.97 Hz, 1H), 7.31−7.26 (m, 3H), 7.42 (d, J = 8.82 Hz, 2H), 7.61 (d, J = 8.48 Hz, 2H), 7.88 (t, J = 1.86 Hz, 1H), 8.99 (s, 1H); MS (ESI) m/z 420, 422 (M − H)$^−$. Anal. (C$_{20}$H$_{16}$BrN$_5$O·0.1C$_6$H$_{14}$·0.1CH$_2$Cl$_2$) C, H, N.

N-[4-(3-Amino-1H-indazol-4-yl)phenyl]-N′-[3-(trifluorometh-yl)phenyl]urea (17n). ^{1}H NMR (DMSO-d_6) δ 6.86 (dd, J = 6.10, 2.03 Hz, 1H), 7.29−7.35 (m, 3H), 7.42 (d, J = 8.81 Hz, 2H), 7.53 (t, J = 7.97 Hz, 1H), 7.58−7.65 (m, 3H), 8.05 (s, 1H), 9.01 (s, 1H), 9.16 (s, 1H). MS (ESI) m/z 412 (M + H)$^+$. Anal. (C$_{21}$H$_{16}$F$_3$N$_5$O·0.7CF$_3$CO$_2$H) C, H, N.

N-(4-(3-Amino-1H-indazol-4-yl)phenyl)-N′-(3-hydroxyphen-l)urea (17o). ^{1}H NMR (DMSO-d_6) δ 5.33 (s, 2H), 6.38 (dd, J = 7.63, 1.86 Hz, 1H), 6.76−6.92 (m, 2H), 6.99−7.14 (m, 2H), 7.26−7.45 (m, 4H), 7.59 (d, J = 8.81 Hz, 2H), 8.65 (s, 1H), 8.80 (s, 1H), 9.31 (s, 1H), 12.11 (s, 1H); MS (ESI) m/z 360 (M + H). Anal. (C$_{20}$H$_{17}$N$_5$O$_2$·0.85CF$_3$CO$_3$H) C, H, N.

N-(4-(3-Amino-1H-indazol-4-yl)phenyl)-N′-(2-fluoro-5-meth-ylphenyl)urea (17p). ^{1}H NMR (DMSO-d_6) δ 2.28 (s, 3H), 6.78−6.85 (m, 1H), 6.87 (dd, J = 6.10, 1.70 Hz, 1H), 7.12 (dd, J = 11.53, 8.48 Hz, 1H), 7.30−7.39 (m, 2H), 7.42 (d, J = 8.81 Hz, 2H), 7.60 (d, J = 8.48 Hz, 2H), 8.01 (dd, J = 7.80, 2.37 Hz, 1H), 8.54 (d, J = 2.71 Hz, 1H), 9.23 (s, 1H); MS (ESI) m/z 376 (M + H)$^+$. Anal. (C$_{21}$H$_{18}$FN$_5$O·0.8CF$_3$CO$_2$H) C, H, N.

N-(4-(3-Amino-1H-indazol-4-yl)phenyl)-N′-(4-fluoro-3-meth-ylphenyl)urea (17q). ^{1}H NMR (DMSO-d_6) δ 2.22 (d, J = 1.70 Hz, 3H), 6.84 (dd, J = 6.10, 1.70 Hz, 1H), 7.06 (t, J = 9.16 Hz, 1H), 7.24−7.45 (m, 6H), 7.59 (d, J = 8.48 Hz, 2H), 8.69 (s, 1H), 8.84 (s, 1H); MS (ESI) m/z 376 (M + H)$^+$. Anal. (C$_{21}$H$_{18}$-FN$_5$O·0.8CF$_3$CO$_3$H) C, H, N.

N-[4-(3-Amino-1H-indazol-4-yl)phenyl]-N′-(3-fluoro-4-meth-ylphenyl)urea (17r). ^{1}H NMR (DMSO-d_6) δ 2.17 (s, 3H), 4.33 (s, 2H), 6.78 (dd, J = 5.42, 2.71 Hz, 1H), 7.05 (dd, J = 8.14, 2.03 Hz, 1H), 7.17 (t, J = 8.65 Hz, 1H), 7.23−7.30 (m, 2H), 7.39 (d, J = 8.48 Hz, 2H), 7.45 (dd, J = 12.54, 2.03 Hz, 1H), 7.58 (d, J = 8.81 Hz, 2H), 8.84 (s, 2H), 11.70 (s, 1H); MS (ESI) m/z 376 (M + H)$^+$. Anal. (C$_{21}$H$_{18}$FN$_5$O·0.6CF$_3$CO$_3$H) C, H, N.

N-[4-(3-Amino-1H-indazol-4-yl)phenyl]-N′-[2-fluoro-5-(trif-luoromethyl)phenyl]urea (17s). ^{1}H NMR (DMSO-d_6) δ 4.33 (s, 2H), 6.79 (dd, J = 5.26, 2.54 Hz, 1H), 7.24−7.31 (m, 2H), 7.42 (m, 3H), 7.52 (m, 1H), 7.61 (d, J = 8.48 Hz, 2H), 8.65 (dd, J = 7.29, 2.20 Hz, 1H), 8.96 (s, 1H), 9.32 (s, 1H), 11.72 (s, 1H); MS (ESI) m/z 430 (M + H)$^+$.

4-Iodo-1-methyl-1H-indazol-3-amine (20a). A mixture of 2-fluoro-6-iodobenzonitrile (**7**; 2.6 g, 10.5 mmol) and methyl hydrazine (5.7 mL, 105 mmol) in n-butanol (60 mL) was stirred at 100−110 °C for 3 h and then cooled to room temperature and concentrated. The residue was partitioned between water and ethyl acetate. The aqueous layer was extracted twice with ethyl acetate. The combined extracts were washed with water and brine, dried (MgSO$_4$), filtered, and concentrated to provide the title compound (2.5 g, 87%). ^{1}H NMR (DMSO-d_6) δ 3.74 (s, 3H), 5.11 (s, 2H), 6.97 (dd, J = 8.48, 7.46 Hz, 1H), 7.35 (d, J = 7.46 Hz, 1H), 7.40 (d, J = 8.48 Hz, 1H); MS (ESI) m/z 274 (M + H)$^+$.

2-(4-Iodo-1H-indazol-3-yl)-1H-isoindole-1,3(2H)-dione (18). A mixture of **8** (1.09 g, 4.21 mmol) and phthalic anhydride (0.75 g,

5.26 mmol) in dioxane (15 mL) was stirred at 110 °C overnight and then concentrated. The residue was triturated from diethyl ether (15 mL) to provide the title compound (0.51 g, 31%). MS (ESI) *m/z* 388 (M + H)$^+$.

2-{4-Iodo-1-[2-(4-morpholinyl)ethyl]-1*H*-indazol-3-yl}-1*H*-isoindole-1,3(2*H*)-dione (19c). A mixture of **18** (100 mg, 0.26 mmol), 4-(2-chloroethyl)morpholine (48 mg, 0.32 mmol), and Na$_2$CO$_3$ (82 mg, 0.77 mmol) in DMF (5 mL) was heated overnight at 80 °C, cooled to room temperature, and partitioned between 1 N HCl (aq) and ethyl acetate. The aqueous layer was separated, basified with 1 N KOH (aq), and extracted twice with ethyl acetate. The combined extracts were washed with water and brine, dried (MgSO$_4$), filtered, and concentrated to provide the title compound (45 mg, 34%). MS (ESI) *m/z* 503 (M + H)$^+$.

4-Iodo-1-[2-(4-morpholinyl)ethyl]-1*H*-indazol-3-amine (20c). A mixture of hydrazine monohydrate (58 μL, 1.2 mmol) and **19c** (120 mg, 0.24 mmol) in ethanol (5 mL) was stirred at 0 °C for 1 h and then at room temperature for 3 h. The mixture was concentrated. The residue was purified by flash column chromatography on silica gel with 5−8% methanol in dichloromethane to provide the title compound (80 mg, 90%). MS (ESI) 373 (M + H)$^+$.

4-(4-Aminophenyl)-1-methyl-1*H*-indazol-3-amine (21a). A mixture of **20a** (2.50 g, 9.16 mmol), 4-(4,4,5,5-tetramethyl-1,3,2-dioxaborolan-2-yl)aniline (**10**; 3.0 g, 13.7 mmol), Pd(PPh$_3$)$_4$ (528 mg, 0.46 mmol), and Na$_2$CO$_3$ (2.9 g, 27.48 mmol) in 1,2-dimethoxyethane (40 mL) and water (10 mL) was heated at 90 °C under a nitrogen atmosphere for 16 h. The mixture was concentrated and partitioned between ethyl acetate and water. The aqueous phase was extracted with ethyl acetate twice. The combined organic layers were washed with brine, dried (MgSO$_4$), filtered, and concentrated. The crude product was purified by flash column chromatography on silica gel with 0−5% methanol in dichloromethane to provide the title compound (1.4 g, 65%). ^{1}H NMR (DMSO-d_6) δ 3.76 (s, 1H), 4.40 (s, 2H), 5.27 (s, 2H), 6.64−6.73 (m, 3H), 7.12 (d, *J* = 8.14 Hz, 2H), 7.24−7.27 (m, 2H); MS (ESI) *m/z* 239 (M + H)$^+$.

N-[4-(3-Amino-1-methyl-1*H*-indazol-4-yl)-phenyl]-N′-(3-methylphenyl)urea (22a). To a solution of **21a** (80 mg, 0.34 mmol) in DMF (3 mL) at 0 °C was added *m*-tolyl isocyanate (43 μL, 0.34 mmol). The mixture was stirred overnight and then partitioned between ethyl acetate. The aqueous phase was extracted with ethyl acetate twice. The combined organic phases were washed water and brine, dried (MgSO$_4$), filtered, and concentrated. The crude product was purified by flash column chromatography on silica gel with 0−3% methanol in dichloromethane to give the title compound (40 mg, 31%). ^{1}H NMR (DMSO-d_6) δ 2.29 (s, 3H), 3.79 (s, 3H), 4.39 (s, 2H), 6.79 (dd, *J* = 6.10, 1.70 Hz, 2H), 7.17 (t, *J* = 7.80 Hz, 1H), 7.24−7.40 (m, 6H), 7.59 (d, *J* = 8.48 Hz, 2H), 8.64 (s, 1H), 8.80 (s, 1H); MS (ESI) *m/z* 372 (M + H)$^+$. Anal. (C$_{22}$H$_{21}$N$_5$O·0.1H$_2$O) C, H, N.

N-{4-[3-Amino-1-(2-hydroxyethyl)-1*H*-indazol-4-yl]phenyl}-N′-(3-methylphenyl)urea (22b). A mixture of **20b** (50 mg, 0.166 mmol), **16b** (75 mg, 0.216 mmol), Pd(PPh$_3$)$_4$ (19 mg, 0.017 mmol), and Na$_2$CO$_3$ (52 mg, 0.498 mmol) in 1,2-dimethoxyethane (3 mL) and water (1 mL) was heated at 90 °C under a nitrogen atmosphere for 16 h. The mixture was concentrated and partitioned between ethyl acetate and water. The aqueous phase was extracted with ethyl acetate twice. The combined organic layers were washed with brine, dried (MgSO$_4$), filtered, and concentrated. The crude product was purified by preparative HPLC to provide the title compound (26 mg, 39%). ^{1}H NMR (DMSO-d_6) δ 2.29 (s, 3H), 3.74 (t, *J* = 5.76 Hz, 2H), 4.20 (t, *J* = 5.59 Hz, 2H), 6.79 (d, *J* = 6.78 Hz, 1H), 6.80 (d, *J* = 7.12 Hz, 1H), 7.17 (t, *J* = 7.63 Hz, 1H), 7.23−7.40 (m, 6H), 7.59 (d, *J* = 8.81 Hz, 2H), 8.65 (s, 1H), 8.80 (s, 1H); MS (ESI) *m/z* 402 (M + H)$^+$. Anal. (C$_{23}$H$_{23}$N$_5$O$_2$·0.7CF$_3$CO$_2$H) C, H, N.

N-{4-[3-Amino-1-(2-morpholin-4-yl-ethyl)-1*H*-indazol-4-yl]-phenyl}-N′-(3-methylphenyl)urea (22c). Compound **22c** was prepared from **20c** using the same procedures as for **22a**. ^{1}H NMR (500 MHz, DMSO-d_6) δ 2.29 (s, 3H), 3.58 (t, *J* = 5.77 Hz, 2H), 3.39−3.88 (m, 8H), 4.55 (t, *J* = 6.39 Hz, 2H), 6.80 (d, *J* = 7.49

Hz, 1H), 6.87 (d, *J* = 6.86 Hz, 1H), 7.17 (t, *J* = 7.80 Hz, 1H), 7.26 (d, *J* = 8.42 Hz, 1H), 7.32 (s, 1H), 7.37−7.41 (m, 3H), 7.48 (d, *J* = 8.11 Hz, 1H), 7.61 (d, *J* = 8.42 Hz, 2H), 8.75 (s, 1H), 8.93 (s, 1H); MS (ESI) *m/z* 471 (M + H)$^+$. Anal. (C$_{27}$H$_{30}$N$_6$O$_2$·2.0CF$_3$CO$_2$H) C, H, N.

N-{4-[3-Amino-1-(2-methoxyethyl)-1*H*-indazol-4-yl]phenyl}-N′-(2-fluoro-5-methylphenyl)urea (22d). Compound **22d** was prepared from **18** using the same procedures as for **22c**. ^{1}H NMR (DMSO-d_6) δ 2.28 (s, 3H), 3.21 (s, 3H), 3.69 (t, *J* = 5.43 Hz, 2H), 4.32 (t, *J* = 5.43 Hz, 2H), 6.77−6.86 (m, 2H), 7.12 (dd, *J* = 11.36, 8.31 Hz, 1H), 7.23−7.35 (m, 1H), 7.40 (d, *J* = 8.48 Hz, 2H), 7.59 (d, *J* = 8.48 Hz, 2H), 8.01 (dd, *J* = 7.80, 2.03 Hz, 1H), 8.54 (d, *J* = 2.37 Hz, 1H), 9.21 (s, 1H); MS (ESI) *m/z* 434 (M + H)$^+$. Anal. (C$_{24}$H$_{24}$N$_5$O$_2$·0.5CF$_3$CO$_2$H·0.5H$_2$O) C, H, N.

2-Fluoro-6-iodo-3-methylbenzoic acid (24a). A solution of 2-fluoro-4-iodo-1-methylbenzene (**23a**; 25 g, 105.9 mmol) in THF (200 mL) was treated dropwise with LDA (2 M solution in THF, 58.5 mL, 116 mmol) at −78 °C. After being stirred at −78 °C for 1 h, the reaction mixture was treated with excess solid carbon monoxide, and stirred overnight while the reaction temperature slowly rose to room temperature. The mixture was concentrated and then partitioned between 4 N NaOH (aq) and diethyl ether. The aqueous phase was adjusted to pH 2 with 2 N HCl (aq) and then extracted three times with ethyl acetate. The combined extracts were washed with water and brine, dried (MgSO$_4$), filtered, and concentrated to provide the title compound (19.4 g, 66%). ^{1}H NMR (DMSO-d_6) δ 2.21 (d, *J* = 2.03 Hz, 3H), 7.14 (t, *J* = 7.97 Hz, 1H), 7.59 (d, *J* = 8.14 Hz, 1H), 13.84 (s, 1H); MS (ESI) *m/z* 279 (M + H)$^+$.

2-Fluoro-6-iodo-3-methylbenzamide (25a). A mixture of **24a** (19.3 g, 69.1 mmol) in thionyl chloride (60 mL) was heated at 80 °C for 3 h, cooled to room temperature, and concentrated. The residue was dissolved in THF (100 mL), treated at 0 °C with concentrated NH$_4$OH (aq; 80 mL), stirred at room temperature overnight, and concentrated. The residue was suspended in water and filtered. The filter cake was washed with water and dried to provide the title compound (18.67 g, 97%). ^{1}H NMR (DMSO-d_6) δ 2.20 (d, *J* = 2.03 Hz, 3H), 7.07 (t, *J* = 8.14 Hz, 1H), 7.55 (d, *J* = 8.14 Hz, 1H), 7.70 (s, 1H), 7.97 (s, 1H); MS (CI) *m/z* 280 (M + H)$^+$.

2-Fluoro-6-iodo-3-methylbenzonitrile (26a). A solution of **25a** (18.6 g, 66.7 mmol) in DMF (190 mL) was treated dropwise with thionyl chloride (24 mL, 333 mmol), heated at 115 °C for 16 h, cooled to room temperature, poured into ice, and extracted three times with ethyl acetate. The combined extracts were washed with water and brine, dried (MgSO$_4$), filtered, and concentrated. The residue was purified by flash column chromatography on silica gel with 25% ethyl acetate in hexanes to provide the title compound (12.35 g, 71%). ^{1}H NMR (DMSO-d_6) δ 2.24 (d, *J* = 2.03 Hz, 3H), 7.44 (t, *J* = 7.97 Hz, 1H), 7.78 (d, *J* = 8.14 Hz, 1H); MS (CI) *m/z* 279 (M + NH$_4$)$^+$.

4-Iodo-7-methyl-1*H*-indazol-3-amine (27a). Compound **27a** was prepared from **26a** using the same procedure as for **8**. ^{1}H NMR (DMSO-d_6) δ 2.33 (s, 3H), 5.02 (s, 2H), 6.74 (d, *J* = 7.46 Hz, 1H), 7.24 (d, *J* = 7.12 Hz, 1H), 11.83 (s, 1H); MS (ESI) *m/z* 273.8 (M + H)$^+$.

4-(4-Aminophenyl)-7-methyl-1H-indazol-3-amine (28a). Compound **28a** was prepared from **27a** and 4-(4,4,5,5-tetramethyl-1,3,2-dioxaborolan-2-yl)aniline (**10**) using the same procedure as for **9**. ^{1}H NMR (DMSO-d_6) δ 2.39 (s, 3H), 4.33 (s, 2H), 5.21 (s, 2H), 6.60 (d, *J* = 6.78 Hz, 1H), 6.99 (d, *J* = 7.80 Hz, 1H), 7.09 (d, *J* = 8.48 Hz, 2H), 11.62 (s, 1H); MS (ESI) *m/z* 239 (M + H)$^+$.

N-[4-(3-Amino-7-methyl-1*H*-indazol-4-yl)phenyl]-N′-(3-methylphenyl)urea (29a). Compound **29a** was prepared from **28a** and *m*-tolyl isocyanate using the same procedure as for **22a**. ^{1}H NMR (DMSO-d_6) δ 2.29 (s, 3H), 2.42 (s, 3H), 6.70 (d, *J* = 7.1 Hz, 1H), 6.80 (d, *J* = 7.5 Hz, 1H), 7.05 (dd, *J* = 7.1, 1.0 Hz, 1H), 7.16 (t, *J* = 7.8 Hz, 1H), 7.25 (d, *J* = 8.5 Hz, 1H), 7.32 (s, 1H), 7.36 (d, *J* = 8.5 Hz, 2H), 7.57 (d, *J* = 8.5 Hz, 2H), 8.63 (s, 1H), 8.77 (s, 1H), 11.75 (s, 1H); MS (ESI) *m/z* 372 (M + H)$^+$.

N-[4-(3-Amino-7-methoxy-1*H*-indazol-4-yl)phenyl]-*N*′-(3-methylphenyl)urea (29b). Compound **29b** was prepared from **23b** using the same procedures as for **29a**. ^{1}H NMR (DMSO-d_6) δ 2.29 (s, 3H), 3.92 (s, 3H), 4.30 (s, 2H), 6.69 (d, J = 7.80 Hz, 1H), 6.78 (d, J = 7.79 Hz, 1H), 6.80 (d, J = 7.46 Hz, 1H), 7.16 (t, J = 7.80 Hz, 1H), 7.25 (m, 1H), 7.31 (s, 1H), 7.34 (d, J = 8.48 Hz, 2H), 7.55 (d, J = 8.82 Hz, 2H), 8.62 (s, 1H), 8.75 (s, 1H), 11.86 (s, 1H); MS (ESI) *m/z* 388 (M + H)$^+$. Anal. ($C_{22}H_{21}N_5O_{20}$·0.4H$_2$O) C, H, N.

N-[4-(3-Amino-7-fluoro-1*H*-indazol-4-yl)phenyl]-*N*′-(3-methylphenyl)urea (29c). Compound **29c** was prepared from **23c** using the same procedures as for **29a**. ^{1}H NMR (DMSO-d_6) δ 2.29 (s, 3H), 6.75 (dd, J = 7.80, 4.41 Hz, 1H), 6.80 (d, J = 7.46 Hz, 1H), 7.15 (m, 2H), 7.25 (m, 1H), 7.32 (s, 1H), 7.37 (d, J = 8.48 Hz, 2H), 7.59 (d, J = 8.48 Hz, 2H), 8.66 (s, 1H), 8.82 (s, 1H); MS (ESI) *m/z* 376 (M + H)$^+$. Anal. ($C_{21}H_{18}FN_5O$·0.4H$_2$O) C, H, N.

N-[4-(3-Amino-7-bromo-1*H*-indazol-4-yl)phenyl]-*N*′-(3-methylphenyl)urea (29d). Compound **29d** was prepared from **23d** using the same procedures as for **29a**. ^{1}H NMR (DMSO-d_6) δ 2.29 (s, 3H), 4.46 (s, 2H), 6.73 (d, J = 7.46 Hz, 1H), 6.80 (d, J = 6.78 Hz, 1H), 7.17 (t, J = 7.63 Hz, 1H), 7.24−7.32 (m, 2H), 7.39 (d, J = 8.48 Hz, 2H), 7.50 (d, J = 7.80 Hz, 1H), 7.60 (d, J = 8.14 Hz, 2H), 8.64 (s, 1H), 8.82 (s, 1H), 12.08 (s, 1H); MS (ESI) *m/z* 434, 436 (M − H)$^-$. Anal. ($C_{21}H_{18}BrN_5O$) C, H, N.

2-Fluoro-6-iodo-3-methoxybenzonitrile (26b). Compound **26b** was prepared from **23b** using the same procedures as for **26a**. ^{1}H NMR (DMSO-d_6) δ 3.89 (s, 3H), 7.36 (t, J = 8.82 Hz, 1H), 7.80 (dd, J = 8.82, 1.36 Hz, 1H); MS (ESI) *m/z* 278 (M + H)$^+$.

2-Fluoro-3-hydroxy-6-iodobenzonitrile (30). A solution of **26b** (148 mg, 0.54 mmol) in dichloromethane (5 mL) was treated at −78 °C dropwise with BBr$_3$ (2.5 mL, 1 M in dichloromethane, 2.5 mmol), warmed to room temperature, stirred for 18 h, poured into water, and extracted with diethyl ether. The extract was dried (MgSO$_4$), filtered, and concentrated. The residue was purified by flash column chromatography on silica gel with 20% ethyl acetate in hexanes to provide the title compound (110 mg, 77%). ^{1}H NMR (DMSO-d_6) 7.09 (t, J = 8.82 Hz, 1H), 7.62 (dd, J = 8.65, 1.53 Hz, 1H), 10.96 (s, 1H); MS (ESI) *m/z* 262 (M − H)$^-$.

3-(2-Dimethylaminoethoxy)-2-fluoro-6-iodobenzonitrile (31a). To a mixture of **30** (830 mg, 3.16 mmol), 2-dimethylaminoethanol (0.317 mL, 3.79 mmol), and PPh$_3$ on resin (3 mmol/g, 2.11 g, 6.32 mmol) in THF (30 mL) at 0 °C was dropwise added diethyl azodicarboxylate (DEAD; 600 μL, 3.79 mmol). The mixture was stirred overnight, while the temperature slowly rose to room temperature, and then filtered. The residue was purified by flash column chromatography on silica gel eluting first with 75% ethyl acetate in hexane and then with 10% methanol in dichloromethane to provide the title compound (834 mg, 79%). ^{1}H NMR (DMSO-d_6) δ 2.20 (s, 6H), 2.63 (t, J = 5.59 Hz, 2H), 4.18 (t, J = 5.76 Hz, 2H), 7.39 (t, J = 8.82 Hz, 1H), 7.77 (dd, J = 8.82, 1.70 Hz, 1H); MS (ESI) *m/z* 335 (M + H)$^+$.

2-Fluoro-6-iodo-3-(2-methoxyethoxy)benzonitrile (31f). A mixture of **30** (104 mg, 0.39 mmol), 1-bromo-2-methoxyethane (88 μL, 0.94 mmol), and K$_2$CO$_3$ (163 mg, 1.54 mmol) in acetone (5 mL) was heated at 60 °C for 18 h, cooled to room temperature, and partitioned between diethyl ether and water. The extract was dried (MgSO$_4$), filtered, and concentrated to provide the title compound (122 mg, 97%). ^{1}H NMR (DMSO-d_6) δ 3.30 (s, 3H), 3.64−3.69 (m, 2H), 4.20−4.28 (m, 2H), 7.37 (t, J = 8.82 Hz, 1H), 7.77 (dd, J = 8.98, 1.53 Hz, 1H).

7-(2-Dimethylaminoethoxy)-4-iodo-1*H*-indazol-3-ylamine (32a). A mixture of the **31a** (834 mg, 2.5 mmol) and hydrazine monohydrate (1.2 mL, 25 mmol) in 5 mL of *n*-butanol was heated at 110 °C for 5 h and then concentrated. The residue was redissolved in ethyl acetate, washed with water and brine, dried over MgSO$_4$, filtered, and purified by flash column chromatography on silica gel eluting with 6% methanol in dichloromethane to provide the title compound (468 mg, 54%). ^{1}H NMR (DMSO-d_6) δ 2.23 (s, 6H), 2.68 (t, J = 5.76 Hz, 2H), 4.17 (t, J = 5.76 Hz, 2H), 4.97 (s, 2H), 6.54 (d, J = 7.80 Hz, 1H), 7.19 (d, J = 7.80 Hz, 1H), 11.90 (s, 1H); MS (ESI) *m/z* 347 (M + H)$^+$.

4-(4-Aminophenyl)-7-(2-dimethylaminoethoxy)-1*H*-indazol-3-ylamine (33a). A mixture of **32a** (468 mg, 1.35 mmol), **10** (326 mg, 1.68 mmol), Pd(PPh$_3$)$_4$ (50 mg, 0.043 mmol), and Na$_2$CO$_3$ (428 mg, 4.05 mmol) in DME (9 mL) and H$_2$O (3 mL) was heated at 85 °C under a nitrogen atmosphere for 16 h and then partitioned between ethyl acetate and water. The aqueous phase was extracted twice with ethyl acetate. The combined organic phases were washed with water and brine, dried (MgSO$_4$), filtered, and concentrated. The residue was purified by flash column chromatography on silica gel eluting with 12% methanol in dichloromethane to provide the title compound (234 mg, 56%). ^{1}H NMR (DMSO-d_6) δ 2.25 (s, 6H), 2.71 (t, J = 5.76 Hz, 2H), 4.20 (t, J = 5.93 Hz, 2H), 4.30 (s, 2H), 5.17 (s, 2H), 6.58 (d, J = 7.80 Hz, 1H), 6.65 (d, J = 8.48 Hz, 2H), 6.74 (d, J = 7.80 Hz, 1H), 7.07 (d, J = 8.14 Hz, 2H), 11.68 (s, 1H); MS (ESI) *m/z* 312 (M + H)$^+$.

N-{4-[3-Amino-7-(2-dimethylamino-ethoxy)-1*H*-indazol-4-yl]phenyl}-*N*′-(3-methylphenyl)urea (34a). Compound **34a** was prepared from **33a** and *m*-tolyl isocyanate using the same procedure as for **22a**. ^{1}H NMR (500 MHz, DMSO-d_6) δ 2.29 (s, 3H), 2.95 (s, 6H), 3.61 (br s, 2H), 4.50 (m, 2H), 6.77 (d, J = 7.63 Hz, 1H), 6.80 (d, J = 7.32 Hz, 1H), 6.90 (d, J = 7.63 Hz, 1H), 7.16 (t, J = 7.78 Hz, 1H), 7.26 (d, J = 8.54 Hz, 1H), 7.33 (s, 1H), 7.36 (d, J = 8.54 Hz, 2H), 7.59 (d, J = 8.54 Hz, 2H), 8.81 (s, 1 H), 8.97 (s, 1H); MS (ESI) MS *m/z* 445 (M + H)$^+$. Anal. ($C_{25}H_{28}N_6O_2$·1.8CF$_3$CO$_2$H) C, H, N.

N-{4-[3-Amino-7-(2-diethylaminoethoxy)-1*H*-indazol-4-yl]phenyl}-*N*′-(3-methylphenyl)urea (34b). Compound **34b** was prepared from **30** using the same procedures as for **34a**. ^{1}H NMR (500 MHz, DMSO-d_6) δ 1.27 (t, J = 7.33 Hz, 6H), 2.29 (s, 3H), 3.34 (br s, 4H), 3.61 (br s, 2H), 4.49 (t, J = 4.80 Hz, 2H), 6.74 (d, J = 7.49 Hz, 1H), 6.80 (d, J = 7.17 Hz, 1H), 6.88 (d, J = 7.80 Hz, 1H), 7.16 (t, J = 7.80 Hz, 1H), 7.26 (d, J = 8.11 Hz, 1H), 7.32 (s, 1H), 7.35 (d, J = 8.42 Hz, 2H), 7.58 (d, J = 8.42 Hz, 2H), 8.72 (s, 1H), 8.87 (s, 1H); MS (ESI) *m/z* 473 (M + H)$^+$. Anal. ($C_{27}H_{32}N_6O_2$·2.0CF$_3$CO$_2$H) C, H, N.

N-{4-[3-Amino-7-(2-pyrrolidin-1-yl-ethoxy)-1*H*-indazol-4-yl]phenyl}-*N*′-(3-methylphenyl)urea (34c). Compound **34c** was prepared from **30** using the same procedures as for **34a**. ^{1}H NMR (500 MHz, DMSO-d_6) δ 1.93 (br s, 2H), 2.07 (br s, 2H), 2.29 (s, 3H), 3.25 (br s, 2H), 3.69 (br s, 4H), 4.48 (t, J = 4.80 Hz, 2H), 6.77 (d, J = 7.80 Hz, 1H), 6.80 (d, J = 7.49 Hz, 1H), 6.90 (d, J = 7.80 Hz, 1H), 7.16 (t, J = 7.80 Hz, 1H), 7.26 (d, J = 8.11 Hz, 1H), 7.33 (s, 1H), 7.36 (d, J = 8.73 Hz, 2H), 7.59 (d, J = 8.73 Hz, 2H), 8.79 (s, 1H), 8.95 (s, 1H); MS (ESI) *m/z* 471 (M + H)$^+$. Anal. ($C_{27}H_{30}N_6O_2$·1.8CF$_3$CO$_2$H) C, H, N.

N-{4-[3-Amino-7-(2-morpholin-4-ylethoxy)-1*H*-indazol-4-yl]phenyl}-*N*′-(3-methylphenyl)urea (34d). Compound **34d** was prepared from **30** using the same procedures as for **34a**. ^{1}H NMR (DMSO-d_6) δ 2.29 (s, 3H), 2.52−2.55 (m, 4H), 2.79 (t, J = 5.76 Hz, 2H), 3.57−3.60 (m, 4H), 4.26 (t, J = 5.76 Hz, 2H), 4.30 (s, 2H), 6.68 (d, J = 7.46 Hz, 1H), 6.80 (d, J = 7.80 Hz, 2H), 7.16 (t, J = 7.80 Hz, 1H), 7.25 (m, 1H), 7.31 (s, 1H), 7.34 (d, J = 8.48 Hz, 2H), 7.55 (d, J = 8.82 Hz, 2H), 8.64 (s, 1H), 8.77 (s, 1H), 11.81 (s, 1 H); MS (ESI) MS *m/z* 487 (M + H)$^+$. Anal. ($C_{27}H_{30}N_6O_3$·0.3H$_2$O) C, H, N.

N-(4-{3-Amino-7-[2-(2-oxopyrrolidin-1-yl)ethoxy]-1*H*-indazol-4-yl}phenyl)-*N*′-(3-methylphenyl)urea (34e). Compound **34e** was prepared from **30** using the same procedures as for **34a**. ^{1}H NMR (DMSO-d_6) δ 1.93 (m, 2H), 2.24 (t, J = 8.14 Hz, 2H), 2.29 (s, 3H), 3.55 (m, 2H), 3.62 (m, 2H), 4.27 (t, J = 5.43 Hz, 2H), 6.73 (d, J = 7.80 Hz, 1H), 6.80 (d, J = 7.12 Hz, 1H), 6.86 (d, J = 7.80 Hz, 1H), 7.16 (t, J = 7.80 Hz, 1H), 7.25 (m, 1H), 7.32 (s, 1H), 7.35 (d, J = 8.48 Hz, 2H), 7.56 (d, J = 8.48 Hz, 2H), 8.64 (s, 1H) 8.78 (s, 1H); MS (ESI) *m/z* 485 (M + H)$^+$.

1-{4-[3-Amino-7-(2-methoxy-ethoxy)-1*H*-indazol-4-yl]-phenyl}-3-m-tolyl-urea (34f). Compound **34f** was prepared from **31f** using the same procedures as for **34a**. ^{1}H NMR (DMSO-d_6) δ 2.29 (s, 3H), 3.35 (s, 3H), 3.76 (dd, J = 5.09, 3.73 Hz, 2H), 4.27 (t, J = 3.05 Hz, 2H), 4.29 (s, 2H), 6.67 (d, J = 7.46 Hz, 1H), 6.79 (d, J = 7.80 Hz, 2H), 7.16 (t, J = 7.63 Hz, 1H), 7.25 (m, 1H), 7.31 (s, 1H), 7.34 (d, J = 8.48 Hz, 2H), 7.55 (d, J = 8.48 Hz, 2H), 8.63 (s,

1H), 8.76 (s, 1H), 11.83 (s, 1H); MS (ESI) MS m/z 432 (M + H)$^+$. Anal. (C$_{24}$H$_{25}$N$_5$O$_3$) C, H, N.

3-(Bromomethyl)-2-fluoro-6-iodobenzonitrile (39). A mixture of **26a** (8.0 g, 30.6 mmol), *N*-bromosuccinimide (NBS; 6.54 g, 36.78 mmol), and benzoyl peroxide (0.5 g) in carbon tetrachloride (100 mL) was heated to reflux for 36 h, during which additional NBS (9.0 g, 50.6 mmol) and benzoyl peroxide (1.0 g) was added in three portions. The suspension was filtered, and the filtrate was concentrated. The residue was purified by flash column chromatography on silica gel with 20% ethyl acetate in hexanes to provide the title compound (4.83 g, 46%). ^{1}H NMR (DMSO-d_6) δ 4.71 (s, 2H), 7.66 (t, $J = 8.14$ Hz, 1H), 7.92 (d, $J = 8.14$ Hz, 1H).

2-Fluoro-6-iodo-3-(4-morpholinylmethyl)benzonitrile (40a). A solution of **39** (710 mg, 2.09 mmol) and morpholine (0.546 mL, 6.25 mmol) in DMF (8 mL) was stirred at room temperature overnight, poured into water, and extracted twice with ethyl acetate. The combined extracts were washed with water and brine, dried (MgSO$_4$), filtered, and concentrated to provide the title compound (710 mg, 98%). ^{1}H NMR (DMSO-d_6) δ 2.33−2.41 (m, 4H), 3.52 (s, 2H), 3.53−3.59 (m, 4H), 7.52 (t, $J = 7.80$ Hz, 1H), 7.87 (d, $J = 8.14$ Hz, 1H); MS (ESI) m/z 347 (M + H)$^+$.

4-Iodo-7-(4-morpholinylmethyl)-1*H*-indazol-3-amine (41a). Compound **41a** was prepared from **40a** using the same procedure as for **32a**. ^{1}H NMR (DMSO-d_6) δ 2.34−2.42 (m, 4H), 3.54−3.60 (m, 4H), 3.58 (s, 2H), 6.85 (d, $J = 7.46$ Hz, 1H), 7.30 (d, $J = 7.12$ Hz, 1H), 11.66 (s, 1H); MS (ESI) m/z 359 (M + H)$^+$.

4-(4-Aminophenyl)-7-(4-morpholinylmethyl)-1*H*-indazol-3-amine (42a). Compound **42a** was prepared from **41a** and 4-(4,4,5,5-tetramethyl-1,3,2-dioxaborolan-2-yl)aniline (**10**) using the same procedure as for **33a**. ^{1}H NMR (DMSO-d_6) δ 2.42 (d, $J = 4.07$ Hz, 4H), 3.58 (m, 4H), 3.65 (s, 2H), 4.36 (s, 2H), 5.24 (s, 2H), 6.66 (dd, $J = 7.80, 4.41$ Hz, 3H), 7.12 (m, 3H), 11.45 (s, 1H); MS (ESI) m/z 324 (M + H)$^+$.

N-{4-[3-Amino-7-(4-morpholinylmethyl)-1*H*-indazol-4-yl]phenyl}-N′-(3-methylphenyl)urea (43a). Compound **43a** was prepared from **42a** and *m*-tolyl isocyanate using the same procedure as for **22a**. ^{1}H NMR (DMSO-d_6) δ 2.29 (s, 3H), 3.20−4.20 (m, 8H), 4.56 (s, 2H), 6.80 (d, $J = 7.12$ Hz, 1H), 6.92 (d, $J = 7.12$ Hz, 1H), 7.17 (t, $J = 7.80$ Hz, 2H), 7.27 (d, $J = 7.23$ Hz, 1H), 7.32 (s, 1H), 7.42 (m, 3H), 7.63 (d, $J = 8.48$ Hz, 2H), 8.79 (s, 1H), 8.98 (s, 1H); MS (ESI) m/z 457 (M + H)$^+$.

N-(4-{3-Amino-7-[(4-methyl-1-piperazinyl)methyl]-1*H*-indazol-4-yl}phenyl)-N′-(3-methylphenyl)urea (43b). Compound **43b** was prepared from **39** using the same procedures as for **43a**. ^{1}H NMR (DMSO-d_6) δ 2.29 (s, 3H), 2.79 (s, 3H), 3.00−3.50 (m, 8H), 3.95 (s, 2H), 6.80 (d, $J = 7.46$ Hz, 1H), 6.84 (d, $J = 7.46$ Hz, 1H), 7.17 (t, $J = 7.63$ Hz, 1H), 7.23−7.29 (m, 2H), 7.32 (s, 1H), 7.39 (d, $J = 8.48$ Hz, 2H), 7.61 (d, $J = 8.81$ Hz, 2H), 8.76 (s, 1H), 8.94 (s, 1H); MS (ESI) m/z 470 (M + H)$^+$. Anal. (C$_{27}$H$_{31}$N$_7$O·3.6CF$_3$CO$_2$H) C, H, N.

Homogeneous Time-Resolved Fluorescence (HTRF) Assays of Receptor Tyrosine Kinases (KDR, CSF1R, cKIT, FLT1, and FLT3). Assays were performed in a total of 40 μL in 96-well Costar black half-volume plates using HTRF technology.[26] Peptide substrate (Biotin-Ahx-AEEEYFFLFA-amide) at 4 μM, 1 mM ATP, enzyme, and inhibitors was incubated for 1 h at ambient temperature in 50 mM Hepes/NaOH pH 7.5, 10 mM MgCl$_2$, 2 mM MnCl$_2$, 2.5 mM DTT, 0.1 mM orthovanadate, and 0.01% bovine serum albumin. Inhibitors were added to the wells at a final concentration of 3.2 nM to 50 μM with 5% DMSO added as cosolvent. The reactions were stopped with 10 μL/well 0.5 M ethylenediaminetetraacetic acid (EDTA) and then 75 μL buffer containing streptavidin-allophycocyanin (prozyme; 1.1 μg/mL) and PT66 antibody europium cryptate (Cis-Bio; 0.1 μg/mL) was added to each well. The plates were read from 1 to 4 h after addition of the detection reagents and the time-resolved fluorescence (665 to 615 ratio) measured using a Packard Discovery instrument. The amount of each tyrosine kinase added to the wells was calibrated to give a control (no inhibitor) to background (prequenched with EDTA) ratio of 10−15 and was shown to be in the low nanomolar concentration range for each kinase. The inhibition of each well was calculated

using the control and background readings for that plate. Inhibition constants are the mean of two determinations performed with seven concentrations of the test compounds.

Enzyme-Linked Imminosorbent Assay (ELISA) of KDR Cellular Phosphorylation. NIH3T3 cells stably transfected with full length human KDR (VEGFR2) were maintained in a Dulbecco's modified Eagle's medium (DMEM) with 10% fetal bovine serum and 500 μg/mL geneticin. KDR cells were plated at 20 000 cells/well into duplicate 96-well tissue culture plates and cultured overnight in an incubator at 37 °C with 5% CO$_2$ and 80% humidity. The growth medium was replaced with serum-free growth medium for 2 h prior to compound addition. Compounds in DMSO were diluted in serum-free growth medium (final DMSO concentration 1%) and added to cells for 20 min prior to stimulation for 10 min with VEGF (50 ng/mL). Cells were lysed by addition of RIPA buffer (50 mM Tris-HCl (pH 7.4), 1% IGEPAL, 150 mM NaCl, 1 mM EDTA, and 0.25% sodium deoxycholate) containing protease inhibitors (Sigma cocktail), NaF (1 mM), and Na$_3$VO$_4$ (1 mM), and placed on a microtiter plate shaker for 10 min. The lysates from duplicate wells were combined and 170 μL of the combined lysate was added to the KDR ELISA plate. The KDR ELISA plate was prepared by adding anti-VEGFR2 antibody (1 μg/well, R&D Systems) to an unblocked plate and incubated overnight at 4 °C. The plate was then blocked for at least 1 h with 200 μL/well of 5% dry milk in phosphate buffered saline (PBS). The plate was washed two times with PBS containing 0.1% Tween 20 (PBST) before addition of the cell lysates. Cell lysates were incubated in the KDR ELISA plate with constant shaking on a microtiter plate shaker for 2 h at room temperature. The cell lysate was then removed and the plate was washed five times with PBST. Detection of phospho-KDR was performed using a 1:2000 dilution of biotinylated 4G10 antiphosphotyrosine (UBI, Lake Placid, NY), incubated with constant shaking for 1.5 h at room temperature and washed five times with PBST, and for detection, a 1:2000 dilution of streptavidin-HRP (UBI, Lake Placid, NY) was added and incubated with constant shaking for 1 h at room temperature. The wells were then washed five times with PBST and K-Blue HRP ELISA substrate (Neogen) was added to each well. Development time was monitored at 650 nm in a SprectrMax Plus plate reader until 0.4−0.5 absorbance units were obtained (approximately 10 min) in the VEGF only wells. Phosphoric acid (1 M) was added to stop the reaction, and the plate was read at 450 nm. Percent inhibition was calculated using the VEGF only wells as 100% controls and wells containing 5 μM pan-kinase inhibitor as 0% controls (no VEGF wells were used to monitor endogenous phosphorylation state of the cells). IC$_{50}$ values were calculated by nonlinear regression analysis of the concentration response curve. Each IC$_{50}$ determination was performed with five concentrations and each assay point was determined in duplicate.

Estradiol-Induced Murine UE Assay. Twelve week old balb/c female mice (Taconic, Germantown, NY) were pretreated with 10 units of Pregnant Mare's Serum Gonadotropin (PMSG; Calbiochem) intraperitoneally (ip) administered 72 and 24 h prior to estradiol. Mice were randomized the day of the experiment. Test compounds were formulated in a variety of vehicles and administered po 30 min prior to stimulation with an ip injection of water soluble 17β-estradiol (20−25 μg/mouse). Animals were sacrificed and uteri removed 2.5 h following estradiol stimulation by cutting just proximal to the cervix and at the fallopian tubes. After the removal of fat and connective tissue, uteri were weighed, squeezed between filter paper to remove fluid and weighed again. The difference between wet and blotted weights represented the fluid content of the uterus. Compound-treated groups were compared to vehicle-treated groups after subtracting the background water content of unstimulated uteri. Experimental group size was five or six.

HT1080 Tumor Growth Inhibition Model. The 1080 human fibrosarcoma cells were obtained from the American Type Tissue Culture Collection and maintained in Dulbecco's Modified Eagle Medium supplemented with 10% fetal bovine serum and antibiotics. For tumor xenograft studies, cells were suspended in PBS, mixed with an equal volume of matrigel (phenol red free) to a final

concentration of 2 million cells/mL, and inoculated (0.25 mL) into the flank of SCID-beige mice. One week after inoculation, tumor-bearing animals were divided into groups ($n = 10$), and administration of vehicle (2% EtOH, 5% Tween 80, 20% PEG 400, 73% saline) or inhibitor at the indicted dose was initiated. Tumor growth was assessed every 2−3 days by measuring tumor size and calculating tumor volume using the formula [length × width^2]/2.

Mouse PK Analysis. Male CD-1 mice weighing 26−30 g (Charles River Labs) were dosed intraveneously via the tail vein or orally by gavage with a metal feeder tube. Dosing solutions were prepared in 2.5% ethanol, 2.5% DMSO, 5% Tween-80, 25% PEG400, and pH 7.4 PBS, for a dosing volume of 10 mL/kg. Blood samples were collected with a heparinized syringe by cardiac puncture following CO_2 asphixiation at specified times. Plasma samples were aliquoted into 96-well plates, and proteins were precipitated using acidified methanol. Supernatants were stored at −20 °C. Sample analyses were performed by LC-MS using a Shimadzu 10A-VP chromatography system with a Waters YMC-AQ 5 cm column. The mobile phase consisted of 45% acetonitrile and 0.1% acetic acid in water, and the flow rate was 0.4 mL/min. Mass detection was accomplished with an ESI equipped LCQ-Duo by ThermoFinnegan. External standards were prepared from spiked control plasma and used to generate a response factor for every study. Limits of detection were between 20 and 50 nM.

Supporting Information Available: Spectral data of urea boronates **16b−s** and synthesis and spectral data of **44−47**. This material is available free of charge via the Internet at http://pubs.acs.org.

References

(1) Carmeliet, P.; Jain, R. K. Angiogenesis in Cancer and Other Diseases. *Nature* **2000**, *407*, 249−257.
(2) Zetter, B. R. Angiogenesis and Tumor Metastasis. *Annu. Rev. Med.* **1998**, *49*, 407−424.
(3) Ferrara, N.; Kerbel, R. S. Angiogenesis as a Therapeutic Target. *Nature* **2005**, *438*, 967−974.
(4) Yancopoulos, G. D.; Davis, S.; Gale, N. W.; Rudge, J. S.; Wiegand, S. J.; Holash, J. Vascular-Specific Growth Factors and Blood Vessel Formation. *Nature* **2000**, *407*, 242−248.
(5) Ullrich, A.; Schlessinger, J. Signal Transduction by Receptors with Tyrosine Kinase Activity. *Cell* **1990**, *61*, 203−212.
(6) Hubbard, S. R.; Till, J. H. Protein Tyrosine Kinases: Structure and Function. *Annu. Rev. Biochem.* **2000**, *69*, 373−398.
(7) Gschwind, A.; Fischer, O. M.; Ullrich, A. The Discovery of Receptor Tyrosine Kinases: Targets for Cancer Therapy. *Nat. Rev. Cancer* **2004**, *4*, 361−370.
(8) Dancey, J.; Sausville, E. A. Issues and Progress with Protein Kinase Inhibitors for Cancer Treatment. *Nat. Rev. Drug Discovery* **2003**, *2*, 296−313.
(9) Bilodeau, M. T.; Fraley, M. E., Hartman, G. D. Kinase Insert Domain-containing Receptor Kinase Inhibitors as Antiangiogenic Agents. *Expert Opin. Invest. Drugs* **2002**, *11* (6), 737.
(10) Bergsland, E. K. Update on Clinical Trials Targeting Vascular Endothelial Growth Factor in Cancer. *Am. J. Health−Syst. Pharm.* **2004**, *61*, Suppl. 5, S12−S20.
(11) Bridges, A. J. Chemical Inhibitors of Protein Kinases. *Chem. Rev.* **2001**, *101*, 2541−2571.
(12) Wood, J. M.; Bold, G.; Buchdunger, E.; Cozens, R.; Ferrari, S.; Frei, J.; Hofmann, F.; Mestan, J.; Mett, H.; O'Reilly, T.; Persohn, E.; Rosel, J.; Schnell, C.; Stover, D.; Theuer, A.; Towbin, H.; Wenger, F.; Woods-Cook, K.; Menrad, A.; Siemeister, G.; Schirner, M.; Thier-auch, K.-H.; Schneider, M. R.; Drevs, J.; Martiny-Baron, G.; Totzke, F.; Marme, D. PTK787/ZK222584, A Novel and Potent Inhibitor of Vascular Endothelial Growth Factor Receptor Tyrosine Kinases, Impairs Vascular Endothelial Growth Factor-induced Responses and Tumor Growth after Oral Administration. *Cancer Res.* **2000**, *60*, 2178−2189.
(13) Skobe, M.; Fusenig, N. E. Tumorigenic Conversion of Immortal Human Keratinocytes through Stromal Cell Activation. *Proc. Natl. Acad. Sci. U.S.A.* **1998**, *95*, 1050−1055.
(14) Lindahl, P.; Johansson, B. R.; Leveen, P.; Betsholtz, C. Pericyte Loss and Microaneurysm Formation in PDGF-B-deficient Mice. *Science* **1997**, *277*, 242−245.
(15) Lin, E. Y.; Nguyen, A. V.; Russell, R. G.; Pollard, J. W. Colony-Stimulating Factor 1 Promotes Progression of Mammary Tumors to Malignancy. *J. Exp. Med.* **2001**, *193*, 727−740.
(16) Stirewalt, D. L.; Radich, J. P. The Role of FLT3 in Haematopoietic Malignancies. *Nat. Rev. Cancer* **2003**, *3*, 650−665.
(17) Demetri, G. D. Targeting c-Kit Mutations in Solid Tumors: Scientific Rationale and Novel Therapeutic Options. *Semin. Oncol.* **2001**, *28*, 19−26.
(18) Adams, J.; Huang, P.; Patrick, D. A Strategy for the Design of Multiplex Inhibitors for Kinase-Mediated Signaling in Angiogenesis. *Curr. Opin. Chem. Biol.* **2002**, *6*, 486−492.
(19) Arteaga, C. L. Molecular Therapeutics: Is One Promiscuous Drug against Multiple Targets Better than Combinations of Molecule-Specific Drugs? *Clin. Cancer Res.* **2003**, *9*, 1231−1232.
(20) Mandel, D. B.; Laird, A. D.; Xin, X.; Louie, S. G.; Christensen, J. G.; Li, G.; Schreck, R. E.; Abrams, T. J.; Ngai, T. J.; Lee, L. B.; Murray, L. J.; Carver, J.; Chan, E.; Moss, K. G.; Naznedar, J. O.; Sukbuntherng, J.; Blake, R. A.; Sun, L.; Tang, C.; Miller, T.; Shirazian, S.; McMahon, G.; Cherrington, J. M. In Vivo Antitumor Activity of SU11248, A Novel Tyrosine Kinase Inhibitor Targeting Vascular Endothelial Growth Factor and Platelet-derived Growth Factor Receptors: Determination of a Phamarcokinetic/Pharmaco-dynamic Relationship. *Clin. Cancer Res.* **2003**, *9*, 327−337.
(21) Wilhelm, S. M.; Carter, C.; Tang, L.; Wilkie, D.; McNabola, A.; Rong, H.; Chen, C.; Zhang, X.; Vincent, P.; McHugh, M.; Cao, Y.; Shujath, J.; Gawlak, S.; Eveleigh, D.; Rowley, B.; Liu, L.; Adnane, L.; Lynch, M.; Auclair, D.; Taylor, I.; Gedrich, R.; Voznesensky, A.; Riedl, B.; Post, L. E.; Bollag, G.; Trail, P. A. BAY 43-9006. Exhibits Broad Spectrum Oral Antitumor Activity and Targets the RAF/MEK/ERK Pathway and Receptor Tyrosine Kinases Involved in Tumor Progression and Angiogenesis. *Cancer Res.* **2004**, *64*, 7099−7109.
(22) Dai, Y.; Guo, Y.; Frey, R. R.; Ji, Z.; Curtin, M. L.; Ahmed, A. A.; Albert, D. H.; Arnold, L.; Arries, S. S.; Barlozzari, T.; Bauch, J. L.; Bouska, J. J.; Bousquet, P. F.; Cunha, G. A.; Glaser, K. B.; Guo, J.; Li, J.; Marcotte, P. A.; Marsh, K. C.; Mosley, M. D.; Pease, L. J.; Stewart, K. D.; Stoll, V. S.; Tapang, P.; Wishart, N.; Davidsen, S. K.; Michaelides, M. Thienopyrimidine Ureas as Novel Potent Multitargeted Receptor Tyrosine Kinase (RTK) Inhibitors. *J. Med. Chem.* **2005**, *48*, 6066−6083.
(23) Dumas, J.; Smith, R. A.; Lowinger, T. B. Recent Developments in the Discovery of Protein Kinase Inhibitors from the Urea Class. *Curr. Opin. Drug Discovery Dev.* **2004**, *7*, 600−616.
(24) Dumas, J. Protein Kinase Inhibitors from the Urea Class. *Curr. Opin. Drug Discovery Dev.* **2002**, *5*, 718−727.
(25) Daniel, H. A.; Tapang, P.; Magoc, T. J.; Pease, L. J.; Reuter, D. R.; Wei, R.-Q.; Li, J.; Guo, J.; Bousquet, P. F.; Ghoreish-Haack, N. S.; Wang, B.; Bukofzer, G. T.; Wang, Y-C.; Stavropoulos, J. A.; Hartandi, K.; Niquette, A. L.; Soni, N.; Johnson, E. F.; McCall, J. O.; Bouska, J. J.; Luo, Y.; Donawho, C. K.; Dai, Y.; Marcotte, P. A.; Glaser, K. B.; Michaelides, M. R. Davidsen, S. K. Preclinical Activity of ABT-869, a Multitargeted Receptor Tyrosine Kinase Inhibitor. *Mol. Cancer Ther.* **2006**, *5*, 995−1006.
(26) Kolb, A. J.; Kaplita, P. V.; Hayes, D. J.; Park, Y.-W.; Pernell, C.; Major, J. S.; Mathis, G. *Drug Discovery Today* **1998**, *3*, 333−342.